中国科学院国家天文台
NATIONAL ASTRONOMICAL OBSERVATORIES ,CHINESE ACADEMY OF SCIENCES

the SILK ROAD PROJECT at NAOC
丝绸之路 计划

University of Heidelberg, Germany

DRAGON star cluster simulations, and how to form an intermediate mass black hole

Rainer Spurzem, and Silk Road Team

(mainly: Kai Wu, Philip Cho, Vahid Amiri, Marcelo Vergara, Francesco Flammini Dotti, Shuo Li, …)

Astronomisches Rechen-Inst., ZAH, Univ. of Heidelberg, Germany

National Astronomical Observatories (NAOC), Univ. of Chinese Academy of Sciences

Kavli Institute for Astronomy and Astrophysics (KIAA), Peking University

spurzem@ari.uni-heidelberg.de https://astro-silkroad.eu spurzem@nao.cas.cn

ARI Colloquium

July 24, 2025

Sverre Aarseth

Univ. Heidelberg

20 July 1934 – 28 December 2024

https://www.ast.cam.ac.uk/news/sverre-aarseth-20-july-1934-28-december-2024

Picture:

Xi Shuang Banna,

Yunnan, SW China

(R.Sp.)

90’s at Institute of Astronomy, Cambridge, UK

Left: Emanuel Vilkoviski,
Pavel Kroupa, Sverre Aarseth, R.Sp.

Below:
Chris Tout, E. Vilkoviski,
Sverre Aarseth

Binary Parallelization in Norway 2001 – not yet successful


Sambaran Banerjee, Ann-Marie Madigan, Sverre Aarseth, Alexei Minz, Oliver Porth, R.Spurzem
Avetis Sadoyan, Matthew Benacquista
MODEST 8a
Heidelberg 2008
Professional VHDL
2008 3 15

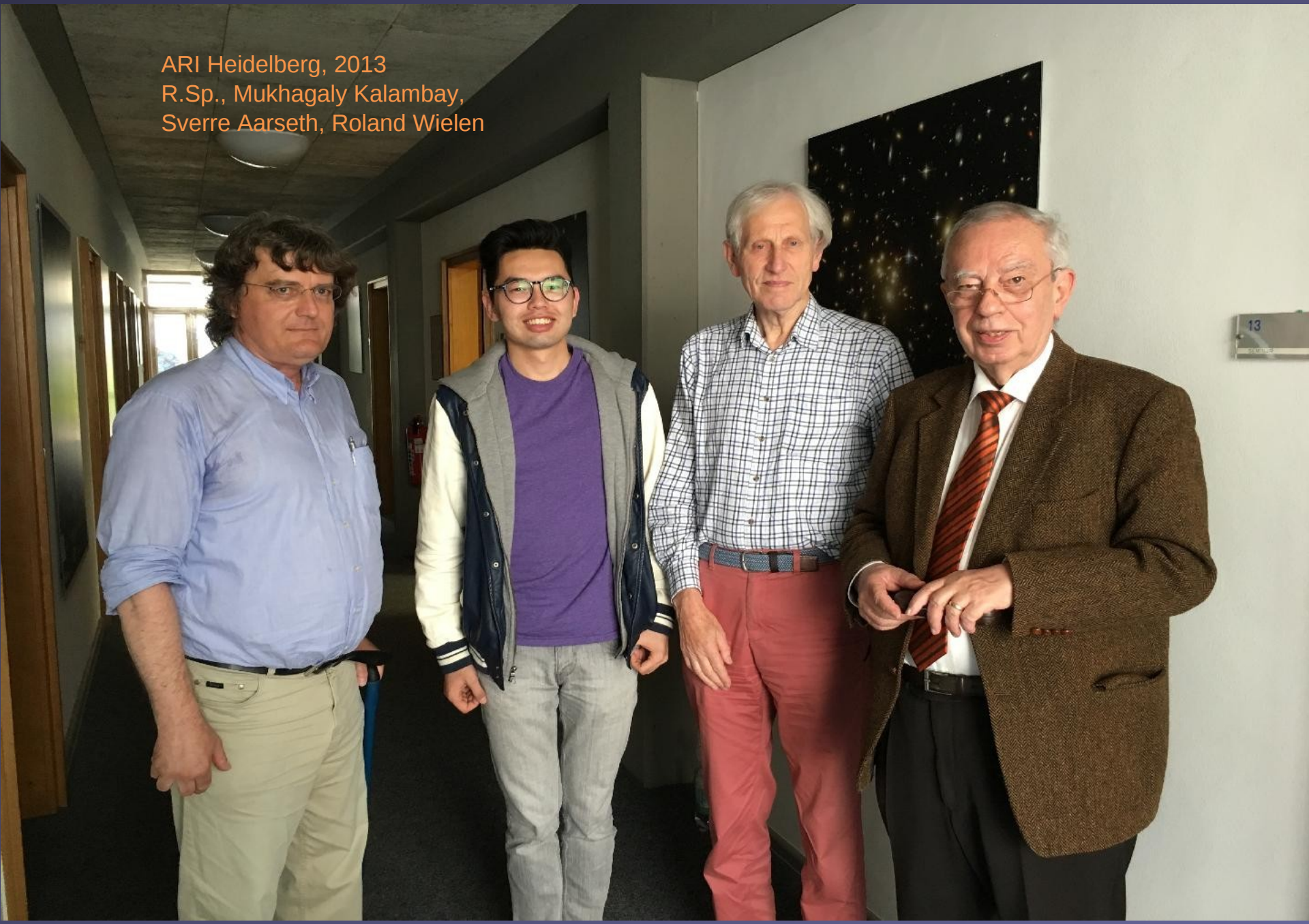
ARI Heidelberg, 2013
R.Sp., Mukhagaly Kalambay,
Sverre Aarseth, Roland Wielen
13

Further Development of
Chain Regularization

IAU Symp. No. 246
Capri, Italy, 2007

Top:
Sverre Aarseth,
Seppo Mikkola

Right:
Sverre Aarseth
Pavel Kroupa
Paulina Assmann


Heidelberg 2018
Work Life Balance
(Pic: A. Just)

Aarseth, Henon, Wielen, 1974, A&A: A comparison of numerical methods for the study of tar cluster dynamics

N-body Codes:

Von Hoerner
Wielen
Aarseth

independent

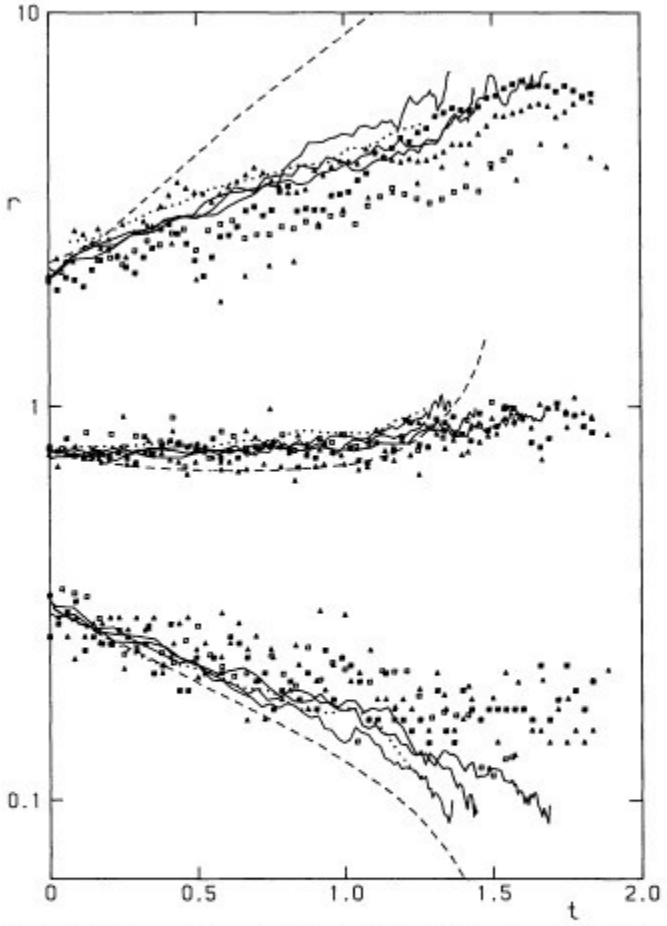

Fig. 1. Radii containing 10%, 50%, 90% of the mass, plotted versus time for a cluster with stars of equal masses. Open triangles and squares: N-body integrations with $N=100$ and $N=250$ (Wielen). Filled triangles and squares: N-body integrations with $N=250$ (Aarseth). Full lines: Monte Carlo models (Hénon). Dotted lines: Monte Carlo model (Shull and Spitzer). Dashed lines: fluid-dynamical model (Larson)

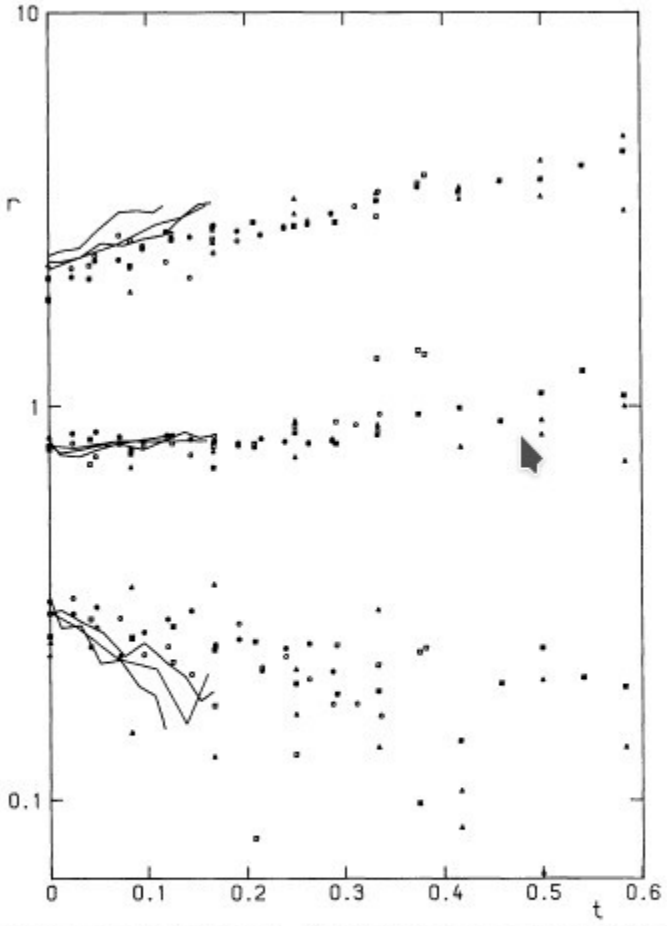

Fig. 2. Radii containing 10%, 50%, 90% of the mass, plotted versus time for a cluster with stars of different masses. Open and filled symbols: N-body integrations with $N=100$ (triangles), $N=250$ (squares), $N=500$ (circles) (Wielen). Full lines: Monte Carlo models (Hénon)

1) **Star Cluster Simulations/ Black Holes/Grav. Waves**
2) Nuclear Star Clusters
3) Code(s) and Hardware
4) Summary and References

Introduction

Kavli Institute for Astronomy and Astrophysics, Peking Univ.

北京大學
PEKING UNIVERSITY

Founded 2008

Astronomisches Rechen-Institut (ARI)
Univ. of Heidelberg, Germany

Founded May 10, 1700

中国科学院国家天文台

NATIONAL ASTRONOMICAL OBSERVATORIES ,CHINESE ACADEMY OF SCIENCES

NAOC/ CAS

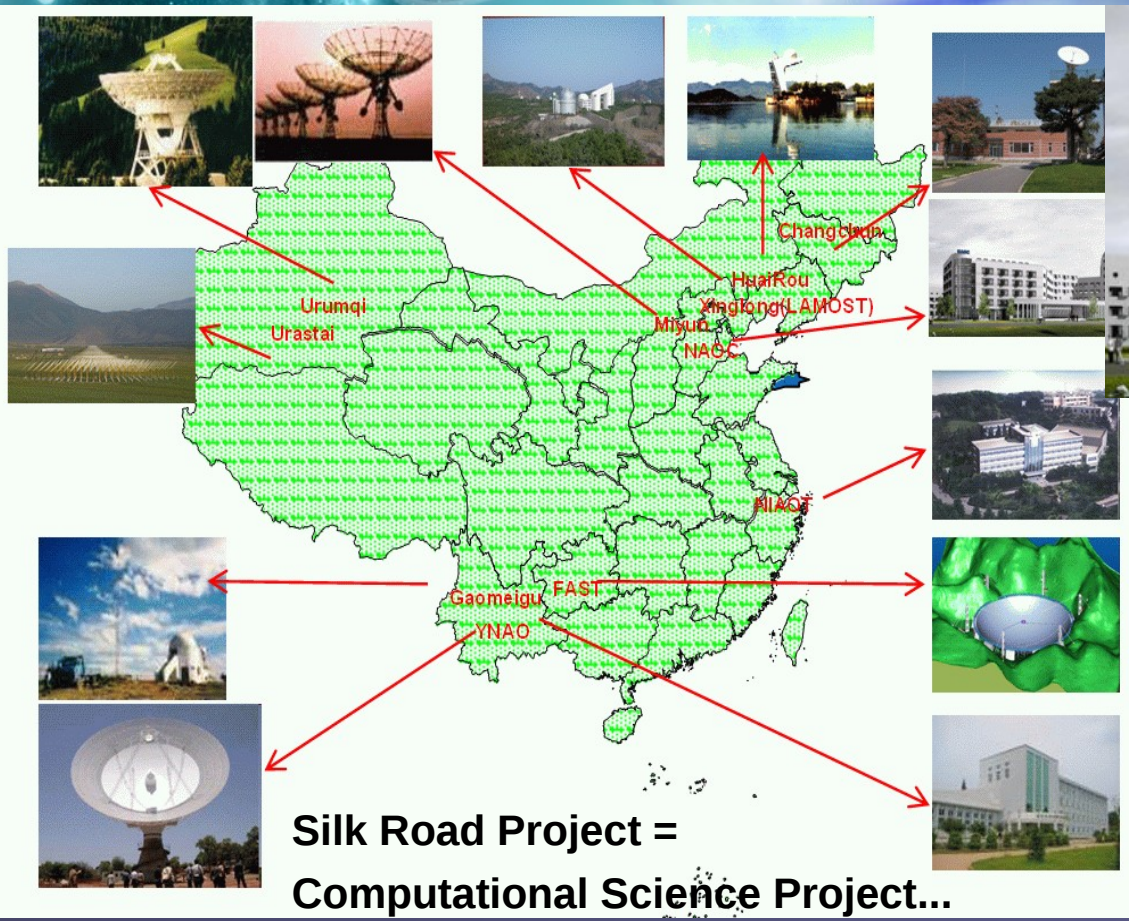

Top: NAOC Headquarter Beijing

Bottom: LAMOST Site

Silk Road Project =

Computational Science Project...

(Credit: X-ray: NASA/CfA/J. Grindlay et al., Optical: NASA/STScI/R. Gilliland et al.)

X-ray binaries

with neutron stars

and black holes

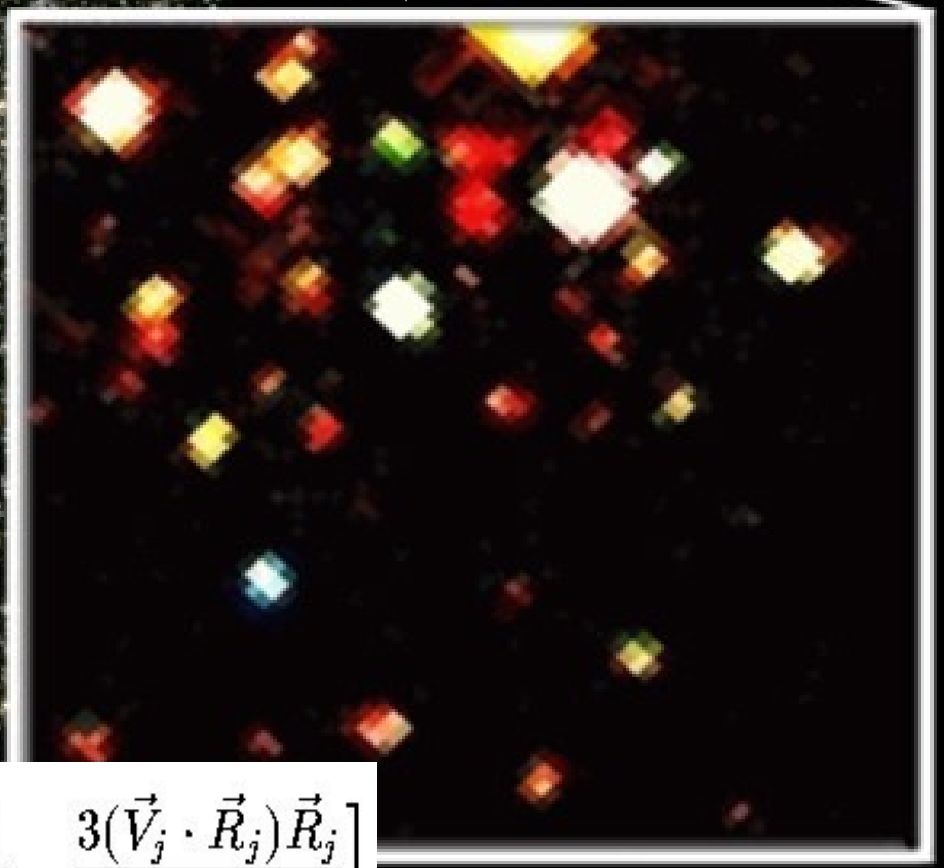

Globular Cluster 47 Tuc

~ one million stars

$$\vec{a}_0 = \sum_j G m_j \frac{\vec{R}_j}{R_j^3} \quad ; \quad \dot{\vec{a}}_0 = \sum_j G m_j \left[\frac{\vec{V}_j}{R_j^3} - \frac{3(\vec{V}_j \cdot \vec{R}_j)\vec{R}_j}{R_j^5} \right]$$

Dynamics of Star Clusters

$$\vec{a}_0 = \sum_j G m_j \frac{\vec{R}_j}{R_j^3} \quad ; \quad \vec{a}_0 = \sum_j G m_j \left[\frac{\vec{V}_j}{R_j^3} - \frac{3(\vec{V}_j \cdot \vec{R}_j)\vec{R}_j}{R_j^5} \right]$$

- $N = \infty$

negative specific Heat

gravothermal Collapse

gravothermal Oscillations

- $N = 3$ $(N = 2, \ldots, \approx 100)$

History

Exponential Instability

Chaos and Resonance

Regularisation

- $N = 10^6$ $(N = 10^4, 10^5)$

Post-Kollaps-Evolution

Binaries

Globular Clusters

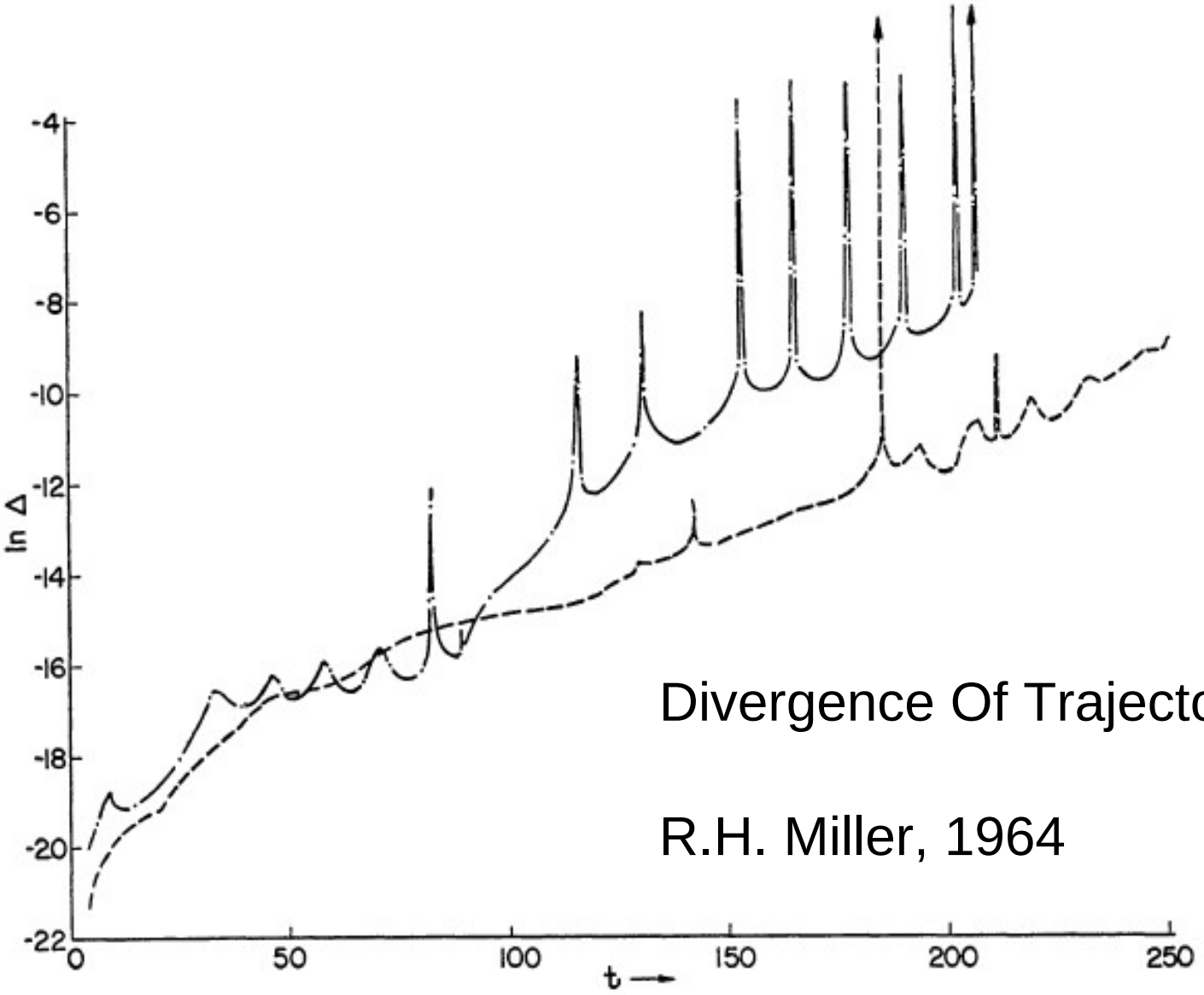

Divergence Of Trajectories

R.H. Miller, 1964

FIG. 2.—Tracks of the separation of phase points for 8-particle stellar dynamical systems. The dashed curve was based on the initial conditions of Section II, while the solid curve results from a different calculation starting from a system that had relaxed from the original atypical condition. The repeated equidistant spikes between $t = 150$ and $t = 220$ are formed by a single long-lived binary pair, which is destroyed in a close collision of one of its members with another star at $t = 225$.

Concept of Shadow Orbits

Quinlan & Tremaine 1992

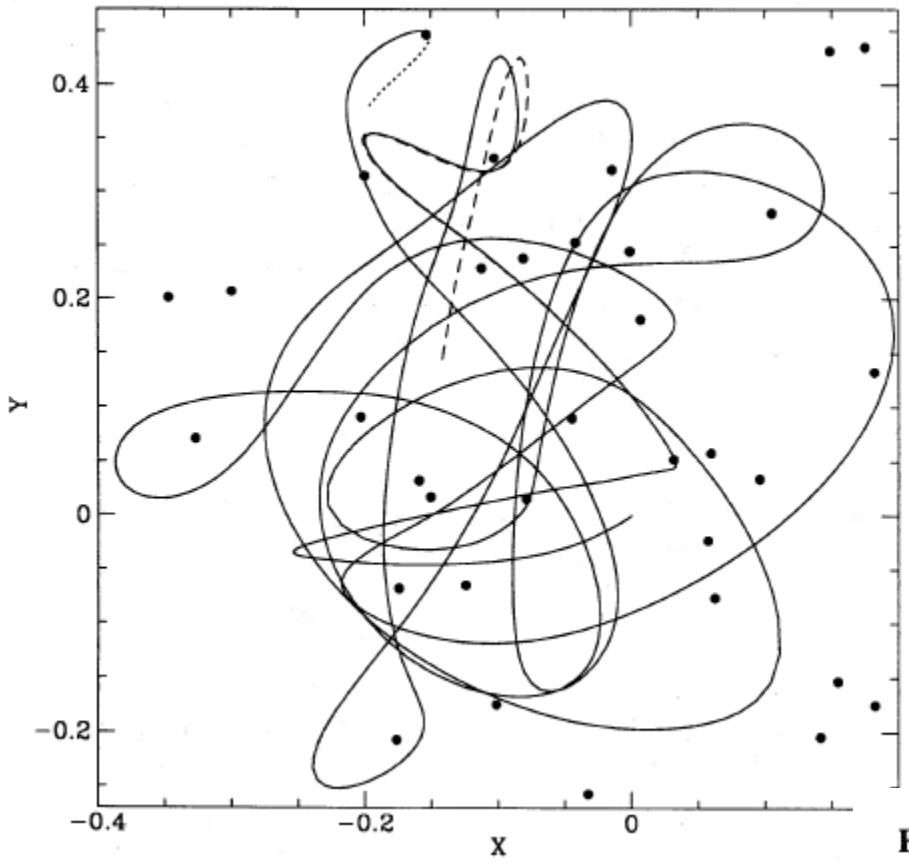

Figure 3. An example of a shadow orbit. The solid line is the projection on to the x–y plane of the noisy orbit of a particle starting at the origin of the cluster in Fig. 1 with velocity $(v_x, v_y, v_z) \simeq (-0.57, -0.46, 0.56)$ integrated for 20.1 time units with accuracy parameter $\eta = 0.027$. The filled circles are the projected positions of the fixed particles in the cluster. The dashed line is an accurate Bulirsch–Stoer integration starting from the same initial conditions, integrated for 3.25 time units. The dotted line is the shadow orbit. The phase-space separation between the shadow and noisy orbits reaches a maximum of 0.042 (resulting mostly from the separation in velocity, not position) near the point $x = 0.033$, $y = 0.051$. The shadow orbit can be seen extending from the end of the noisy orbit at the top of the figure (because the shadow orbit has been plotted for a slightly longer time interval).

Concept of Shadow Orbits

Quinlan & Tremaine 1992

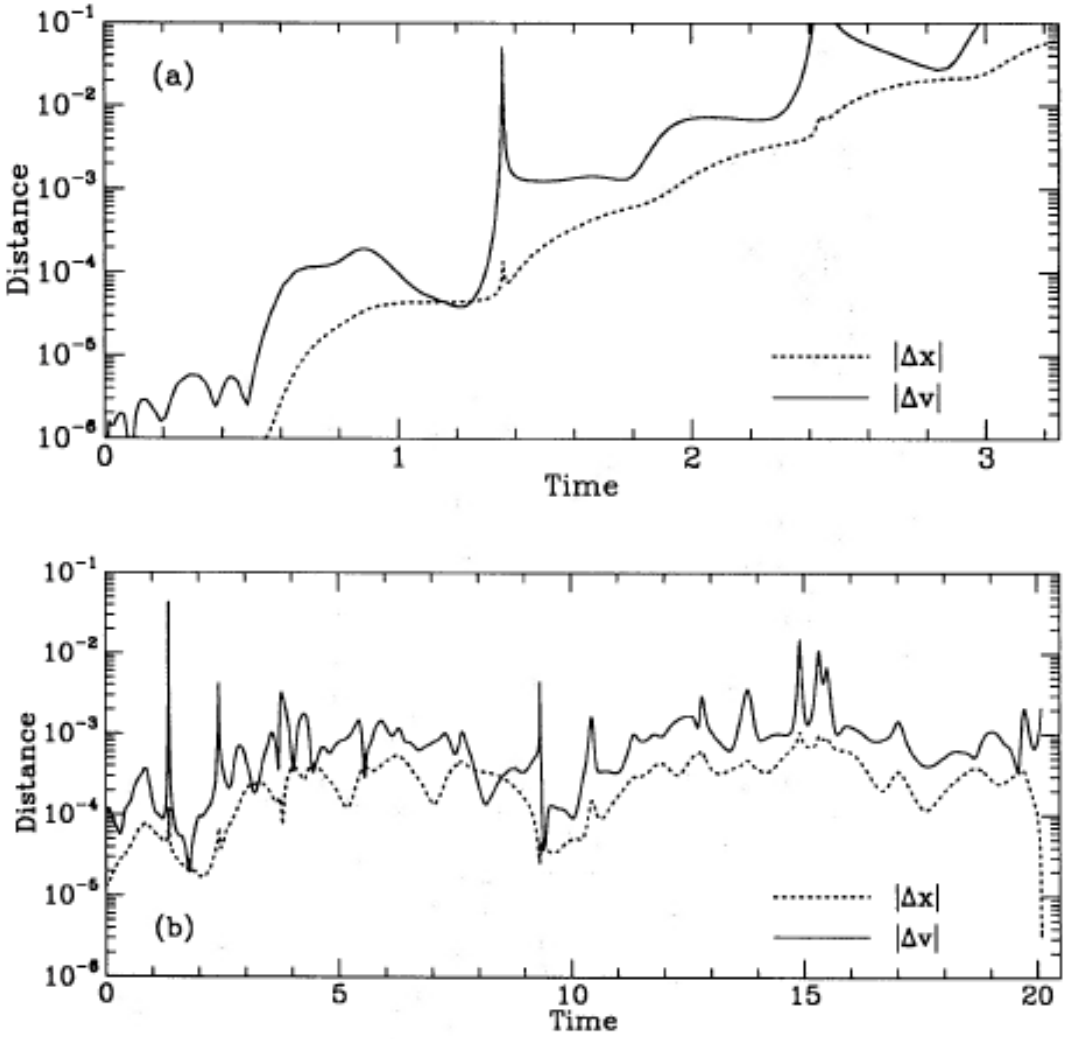

Figure 4. Phase-space separation between the orbits of Fig. 3: (a) separation between the noisy and accurate orbits; (b) separation between the noisy and shadow orbits.

Dynamics of Star Clusters: Gas Sphere Model

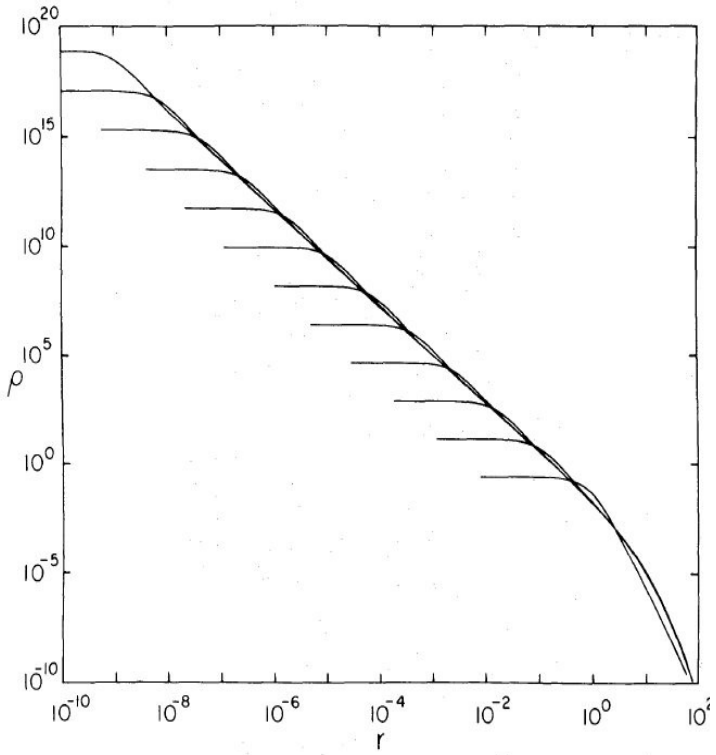

Cohn (1980): Direct Fokker-Planckj model

Core Collapse

Gravothermal Catastrophe

Bettwieser & Sugimoto 1984:

Gravothermal Oscillations by

energy generation from binaries

(cf. nuclear stellar energy generation)

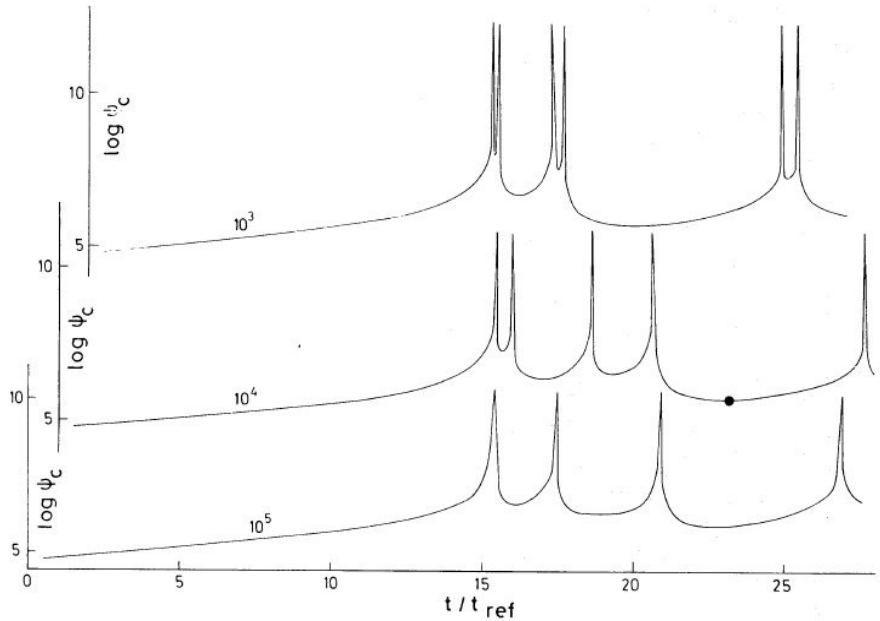

Figure 1. The 'central' density ψ_c is plotted against the non-dimensional time t/t_{ref} for $k = 2$ models with three different values of C as attached to each curve. Note, that if they were plotted with the same ordinate they would be close to each other despite the great differences in C. The model indicated with a filled circle will be compared with King's model in Section 4.2.

3-body Encounters Starlab Simulation (S.L.W. McMillan)

http://www.physics.drexel.edu/~steve/

-> Three-Body-Problem

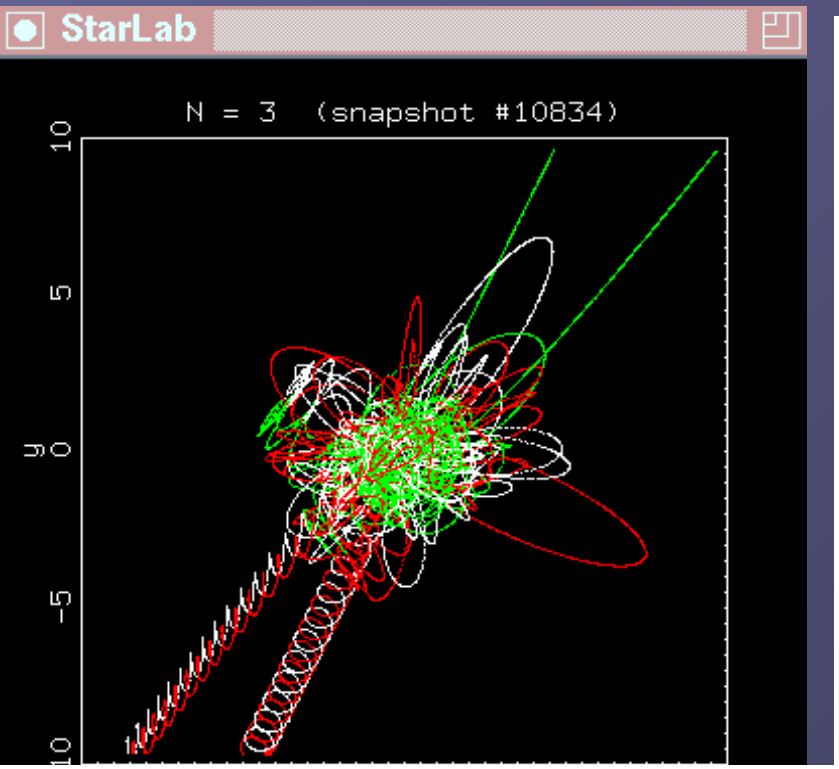

Gravothermal Oscillations - Attractor in Phase Space

Spurzem 1994, Giersz & Spurzem 1994

Amaro-Seoane, Freitag & Sp. 2004

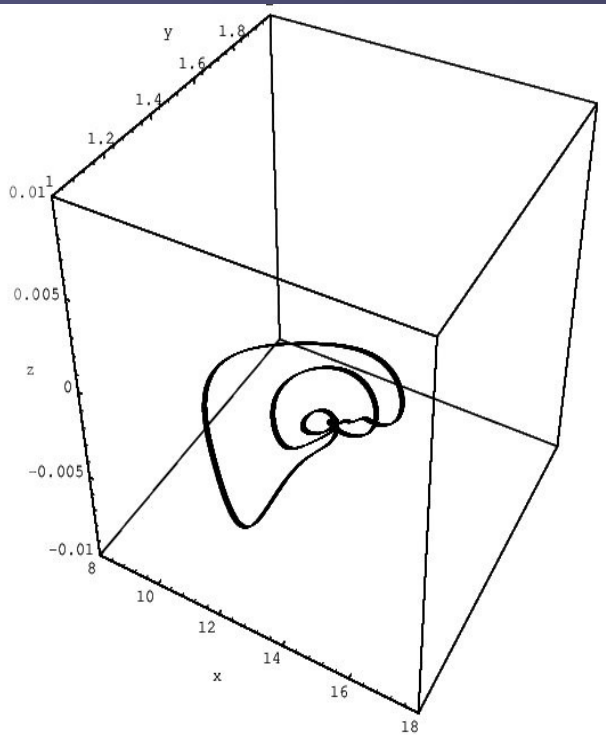

Mon. Not. R. astr. Soc. (1991) **252**, 177–189

Fig. 3:

-dimensional attractor for $N = 100.000$ system, $x = \sigma_c'$, $z = \xi$.

Gravothermal instability of anisotropic self-gravitating gas spheres: singular equilibrium solution

R. Spurzem [1,2,3]

[1] *Institut für Theoretische Physik und Sternwarte, University of Kiel, Olshausenstraße 40, D-2300 Kiel, Germany*
[2] *Institut für Astronomie und Astrophysik, University of Würzburg, Am Hubland, D-8700 Würzburg, Germany*
[3] *Universitätssternwarte Göttingen, Geismarlandstraße 11, D-3400 Göttingen, Germany*

Follow-Up of Angeletti & Giannone and Larson

Dynamics of Star Clusters

(compare gaseous model with direct N-body integration)

(Spurzem & Aarseth 1996)

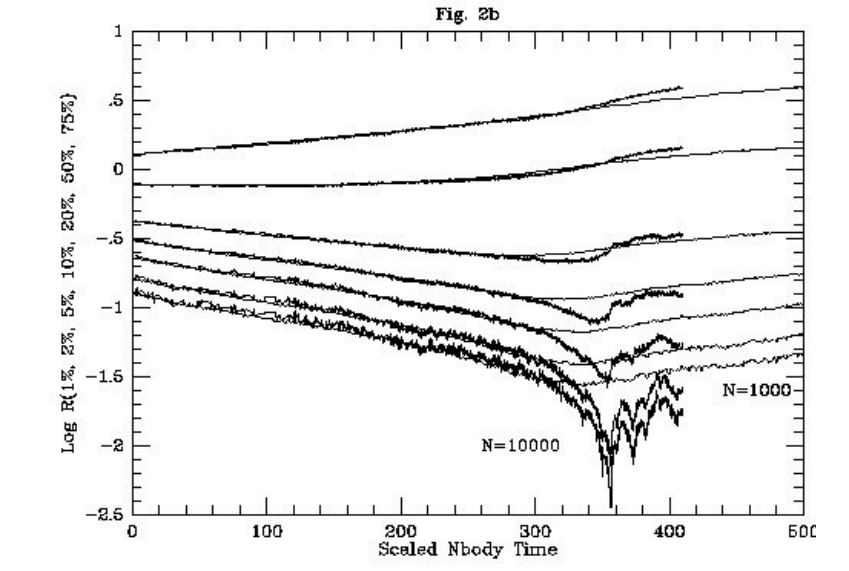

N-Body / N-Body

In spherical symmetry

(Giersz & Spurzem 1994)

(now in Binney/Tremaine)

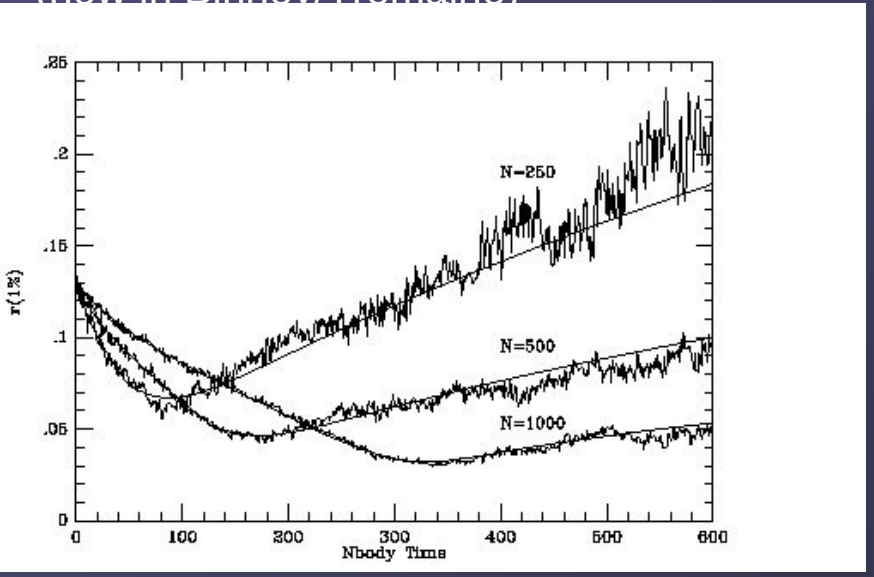

N-Body / Fokker-Planck

...but...

Dynamics of (Rotating) Star Clusters

Fokker-Planck N-Body Comparison

Dissolution of Star Cluster in Tidal Field

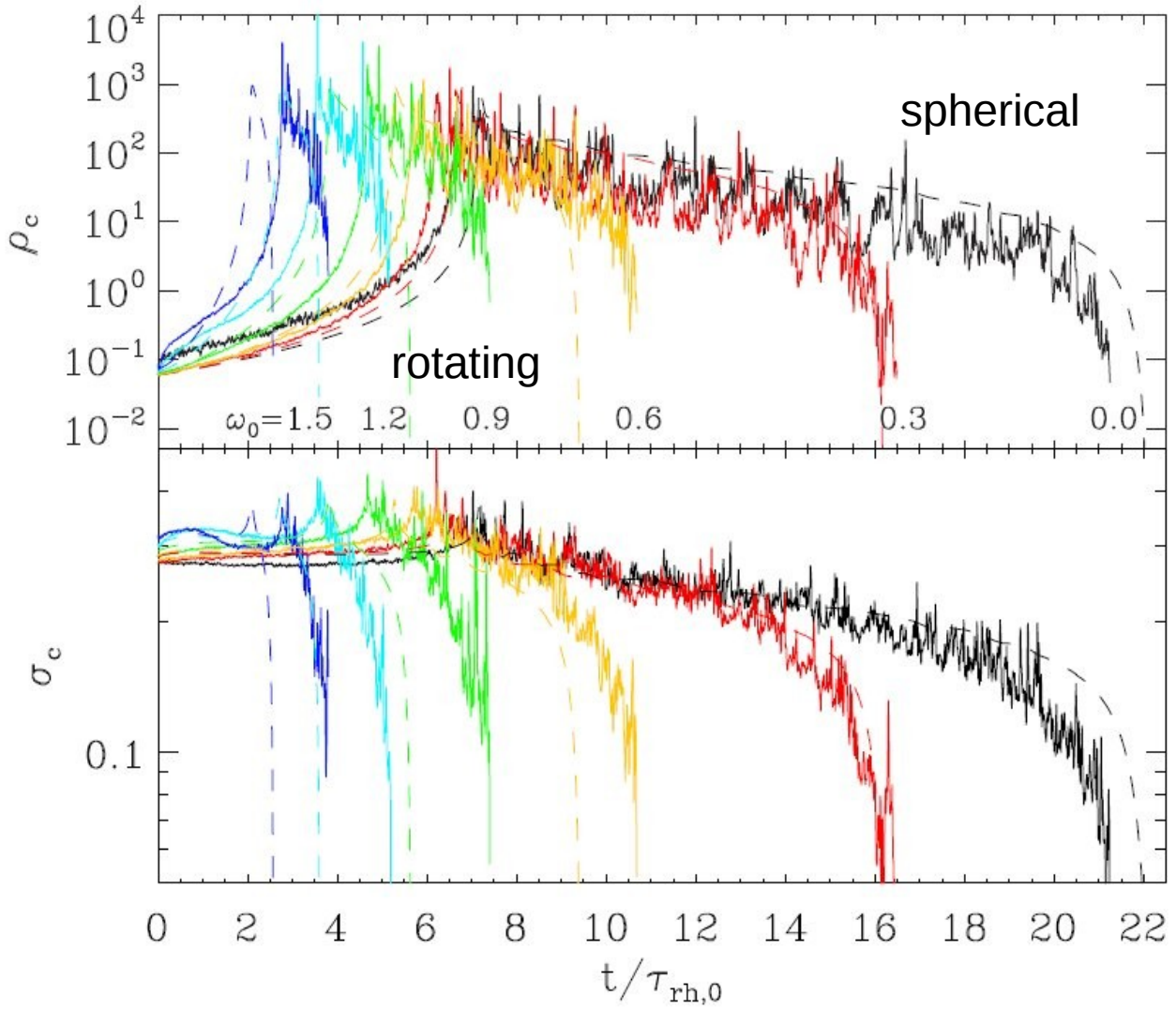

Kim, Yoon, Lee, Spurzem, 2008, MNRAS

Hong, Kim, Lee, Spurzem, 2013, MNRAS

Three Phases in Cluster Dissolution:

1) Core Collapse (Encounters)

2) Post-Collapse Steady Evaporation (Encount)

3) Dynamic final dissolution

DRAGON I Simulation

DRAGON Simulation

http://silkroad.zah.uni-heidelberg.de/dragon/

https://github.com/nbody6ppgpu

Also in: https://www.punch4nfdi.de/

One million stars direct simulation,

biggest and most realistic direct N-Body simulation of globular star clusters.

With stellar mass function, single and binary stellar evolution, regularization of close encounters, tidal field (NBODY6++GPU).

(NAOC/Silk Road/MPA collaboration).

Wang, Spurzem, Aarseth, Naab et al. MNRAS, 2015

Wang, Spurzem, Aarseth Naab, et al. MNRAS 2016

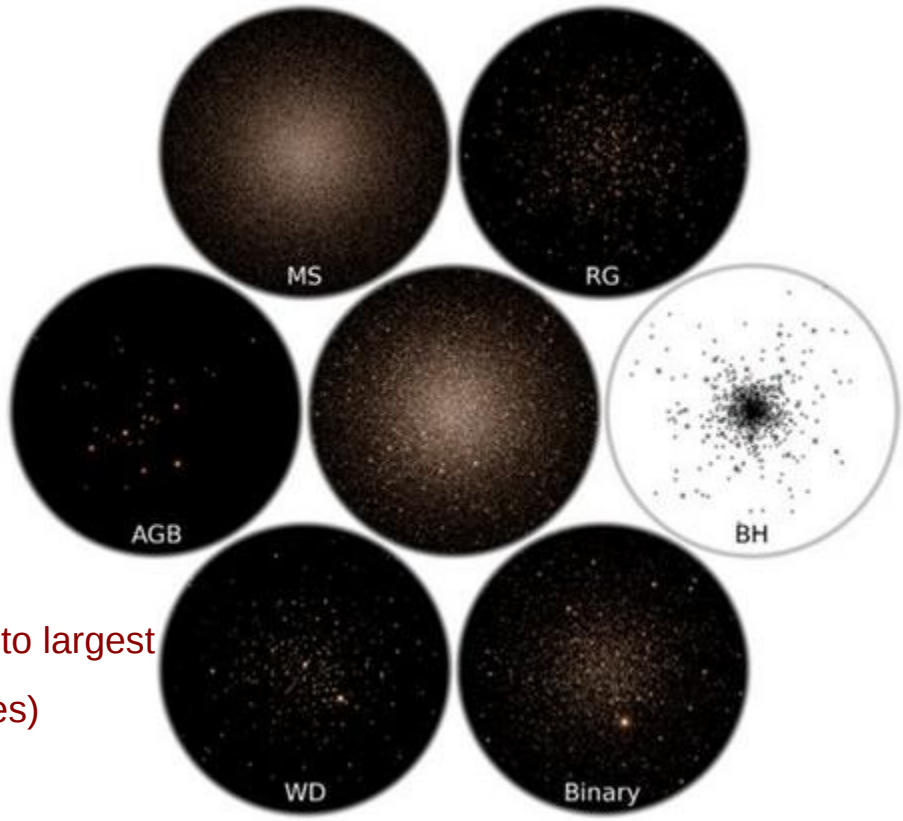

Number of Floating Point Operations (~1M bodies) similar to largest

Cosmological simulations (Millennium, Illustris, ~10^{10} bodies)

天龙星团模拟：百万数量级恒星、黑洞和引力波

Dragon Star Cluster Simulations: Millions of Stars; black holes and gravitational waves

- First realistic globular star cluster model with million stars *(Wang, Spurzem, Aarseth, …, Berczik, Kouwenhoven, … MNRAS 2015, 2016)*
- Synthetic CMD (right side) with zero photometric errors, different ages shown
- Black hole binary mergers occur as observed by LIGO. Our grav. waveforms computed from simulation (right side). (Only inspiral plotted not ringdown.)
- GPU accelerated supercomputers laohu in NAOC and hydra of Max-Planck (MPCDF) in Germany needed!

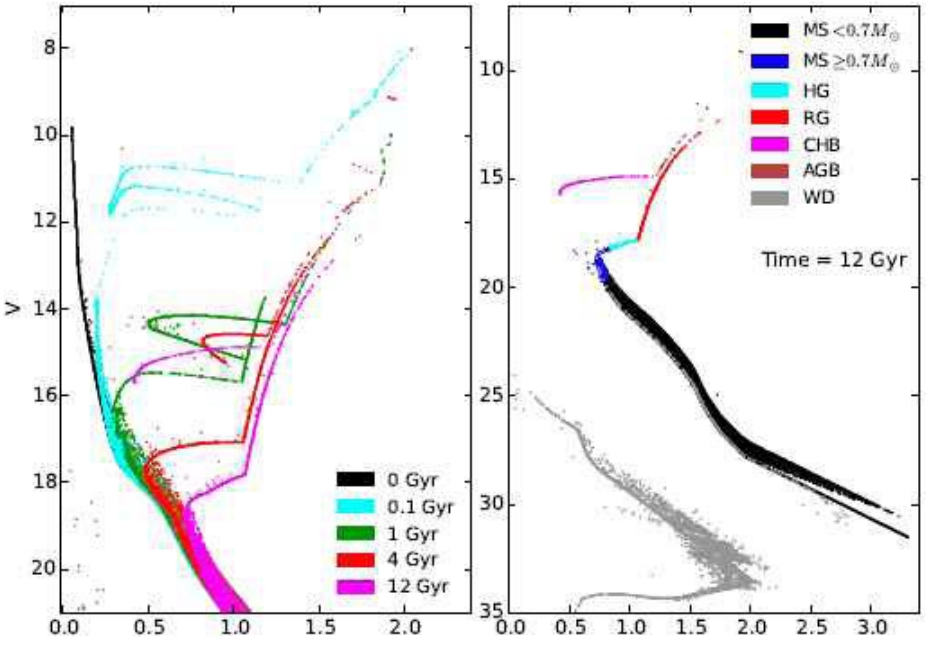

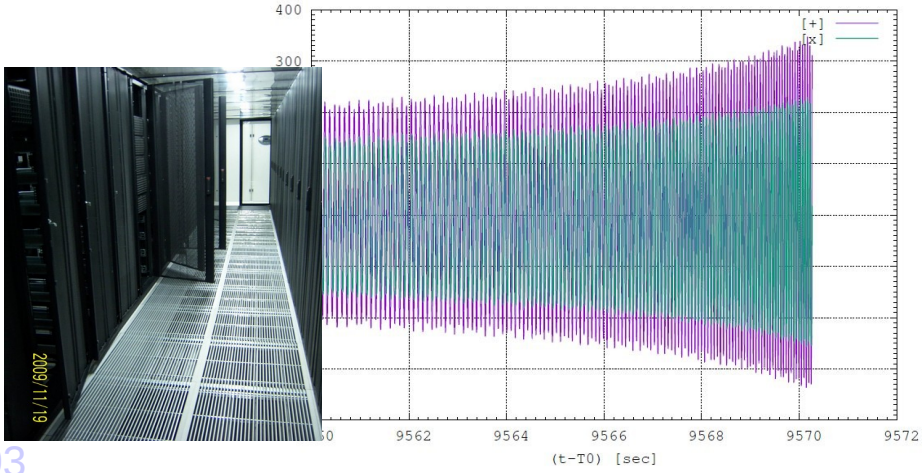

http://www.mpa-garching.mpg.de/328833/hl201603

DRAGON II Simulations

DRAGON-II Simulations – Paper III

using NBODY6++GPU

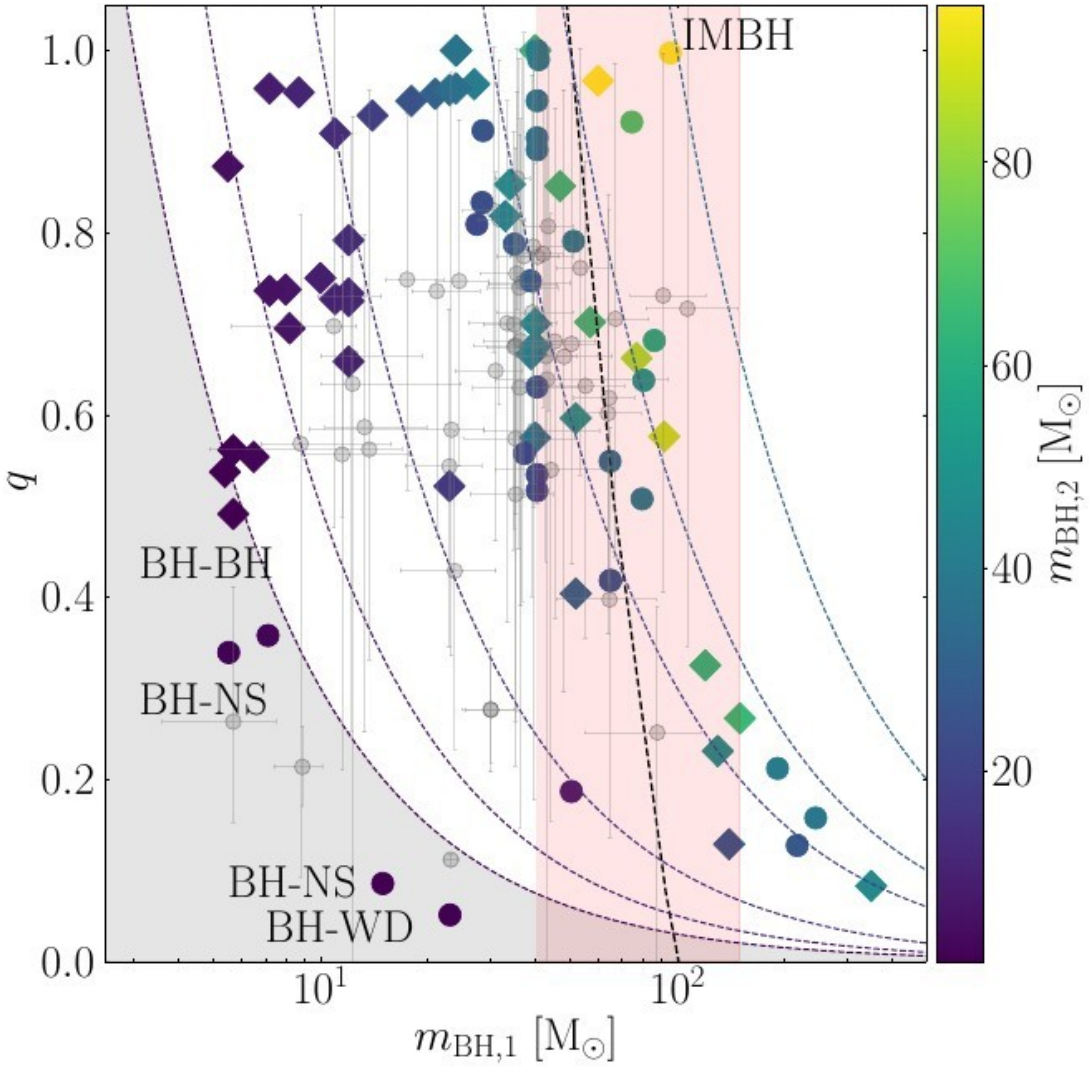

Arca Sedda et al. 2023ab, 2024: MNRAS

19 models, up to 1 million stars, up to 33% initial hard binaries

Compact Object Mergers

Compared with LIGO-Virgo GWTC-3 catalogue (grey symbols)

Mass ratio q vs. primary mass m1; colour code:

secondary mass m2

grey shade: neutron star involved

red Shade: mass gap

DRAGON I Simulation: Wang, Spurzem, Aarseth, et al. 2015, 2016

DRAGON II Simulation: Arca Sedda, Kamlah, Spurzem, et al. 2023, 2024ab

DRAGON III Simulation: Wu et al. 2025, in prep., and DRAGON Data Release

The Future - DRAGON III 1m – 8m (16m?)

ARI Colloquium Kai Wu, July 10, 2025

Young Dense Clusters

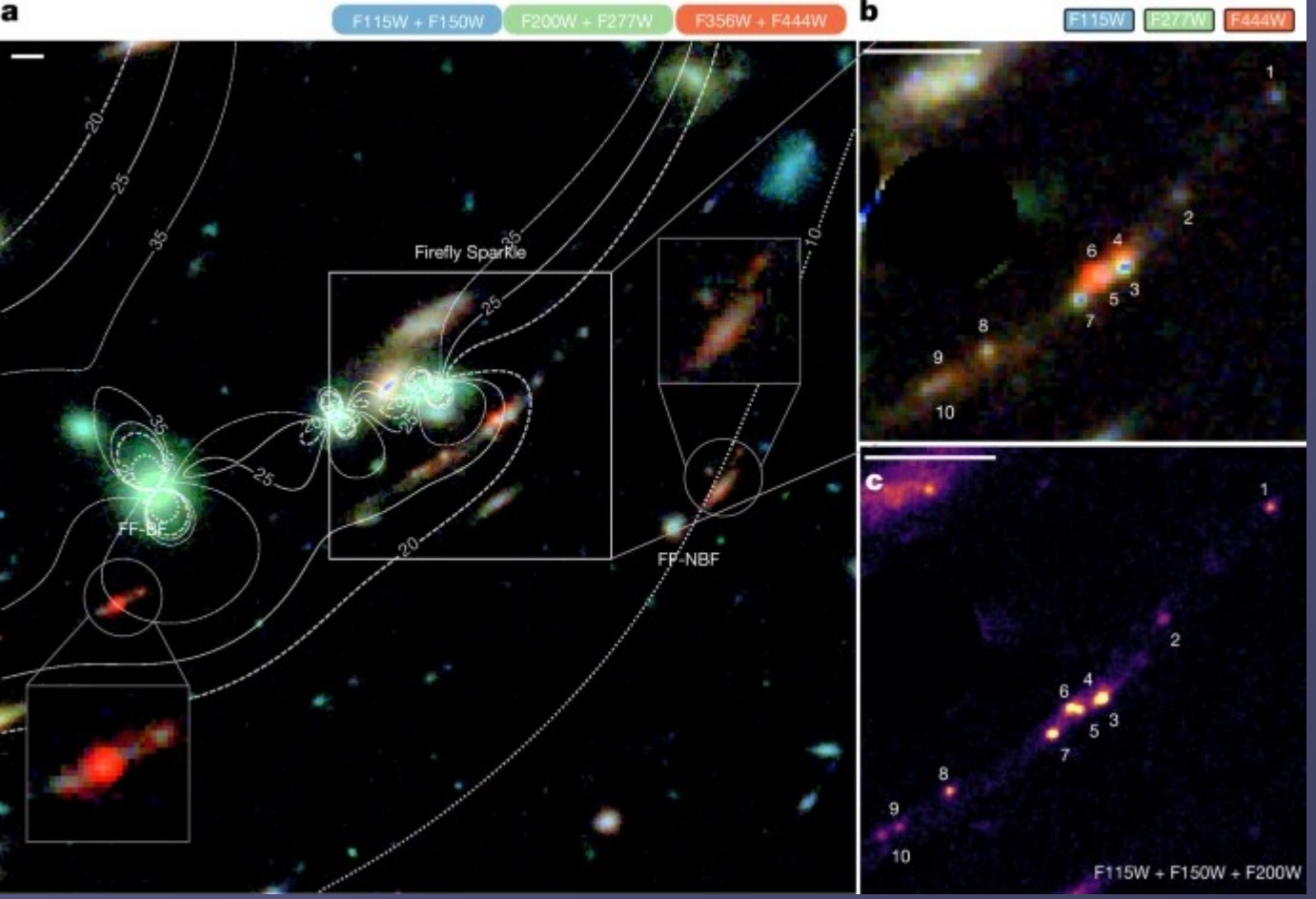

Globular Clusters in the Young Universe I

c, Combined short wavelength (F115W + F150W + F200W) image of the Firefly Sparkle, in which the distinct clusters can be seen. Scale bars, 1″.

NATURE 636, pages 332–336 (2024), Mowla et al. Dec. 2024: The most distant galaxies detected were seen when the Universe was a scant 5% of its current age. At these times, progenitors of galaxies such as the Milky Way were about 10,000 times less massive. … Here we present JWST observations of a strongly lensed galaxy at zspec = 8.296 ± 0.001, showing massive star clusters (the Firefly Sparkle)...The Firefly Sparkle exhibits traits of a young, gas-rich galaxy in its early formation stage. The mass of the galaxy is concentrated in 10 star clusters (49–57% of total mass), with individual masses ranging from $10^5 M_\odot$ to $10^6 M_\odot$. These unresolved clusters have high surface densities ($>10^3 M_\odot\ pc^{-2}$), exceeding those of Milky Way globular clusters and young star clusters in nearby galaxies. The central cluster shows … a top-heavy initial mass function. These observations provide our first spectrophotometric view of a typical galaxy in its early stages, in a 600-million-year-old Universe.

Work in Progress: Very Massive Stars, ... Black Holes, Relativistic Dynamics

Astronomy & Astrophysics manuscript no. output
March 23, 2025

Submitted A&A May 2025

©ESO 2025

Rapid formation of a very massive star >50000 $M_\odot$ and subsequently an IMBH from runaway collisions

Direct N-body and Monte Carlo simulations of dense star clusters

Marcelo C. Vergara[1⋆], Abbas Askar[2⋆⋆], Albrecht W. H. Kamlah[3,1], Rainer Spurzem[1,4,5], Francesco Flammini Dotti[1], Dominik R.G. Schleicher[6], Manuel Arca Sedda[7,8,9,10], Arkadiusz Hypki[11,2], Mirek Giersz[2], Jarrod Hurley[12,13], Peter Berczik[2,14,15], Andres Escala[16], Nils Hoyer[3,17,18], Nadine Neumayer[3], Xiaoying Pang[19,20], Ataru Tanikawa[21,22], Renyue Cen[23,24], and Thorsten Naab[25]

(Affiliations can be found after the references)

Received September 15, 1996; accepted March 16, 1997

ABSTRACT

Context. Simulation of a massive young star cluster using NBODY6++GPU and MOCCA is presented. The cluster is initially more concentrated than previously published models, with one million stars, an initial mass of $5.86 \cdot 10^5$ $M_\odot$, and an initial half-mass radius of $r_{h,i} = 0.1$ pc.
Aims. Analyse the growth of a very massive star (VMS) and the characteristic properties of the collisions leading to its growth. It also seeks to understand the formation of an intermediate-mass black hole (IMBH) through direct stellar collisions in the central regions of a star cluster.
Methods. Both direct N-body and Monte Carlo simulations, include an updated of the standard single and binary stellar evolution packages (SSE and BSE) for massive and VMS, particularly regarding stellar radii, rejuvenation, and mass loss during stellar collisions, providing approximations for stellar radii, rejuvenation, and mass loss during collisions. These updates serve as reasonable extrapolations for very massive stars, though future detailed models may require further refinement.
Results. The simulations reveal that a VMS of approximately 50,000 $M_\odot$ forms through a large number of direct stellar collisions within about 5 Myr in the central regions of the star cluster. This VMS eventually becomes an IMBH.
Conclusions. Our model shows that dense stellar environments are ideally suited to forming massive black holes through stellar collisions. The findings have implications for the formation of black hole seeds in star clusters and are relevant to recent JWST observations of young star clusters in the early Universe.

Key words. star clusters: globular clusters–stars: massive–methods: numerical

Work in Progress:
Very Massive Stars, ... Black Holes,
Relativistic Dynamics

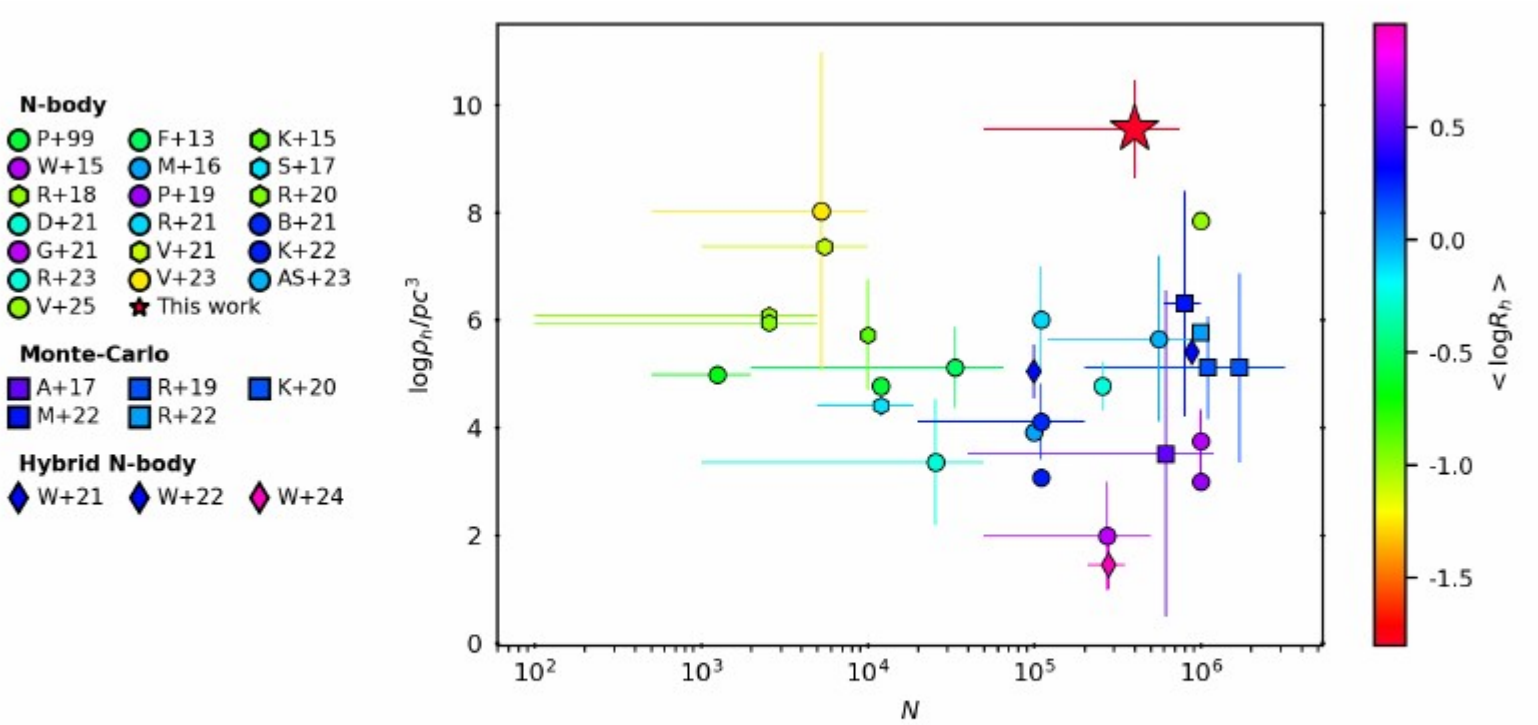

Fig. 1. Initial half-mass density ρ_h, computed at the initial half-mass radius r_h, is expressed as a function of the initial number of stars N. Figure has been reproduced from Arca Sedda et al. (2023, 2024a,b) and has been adapted to include a color bar with the logarithm of the average half-mass radius. Besides we include others simulations and the new ones presented in this paper.

Fast Intermediate Mass Black Hole Formation By Stellar Collisions in Dense Star Cluster

Vergara et al: Rapid formation of a VMS and subsequently an IMBH in a dense star cluster

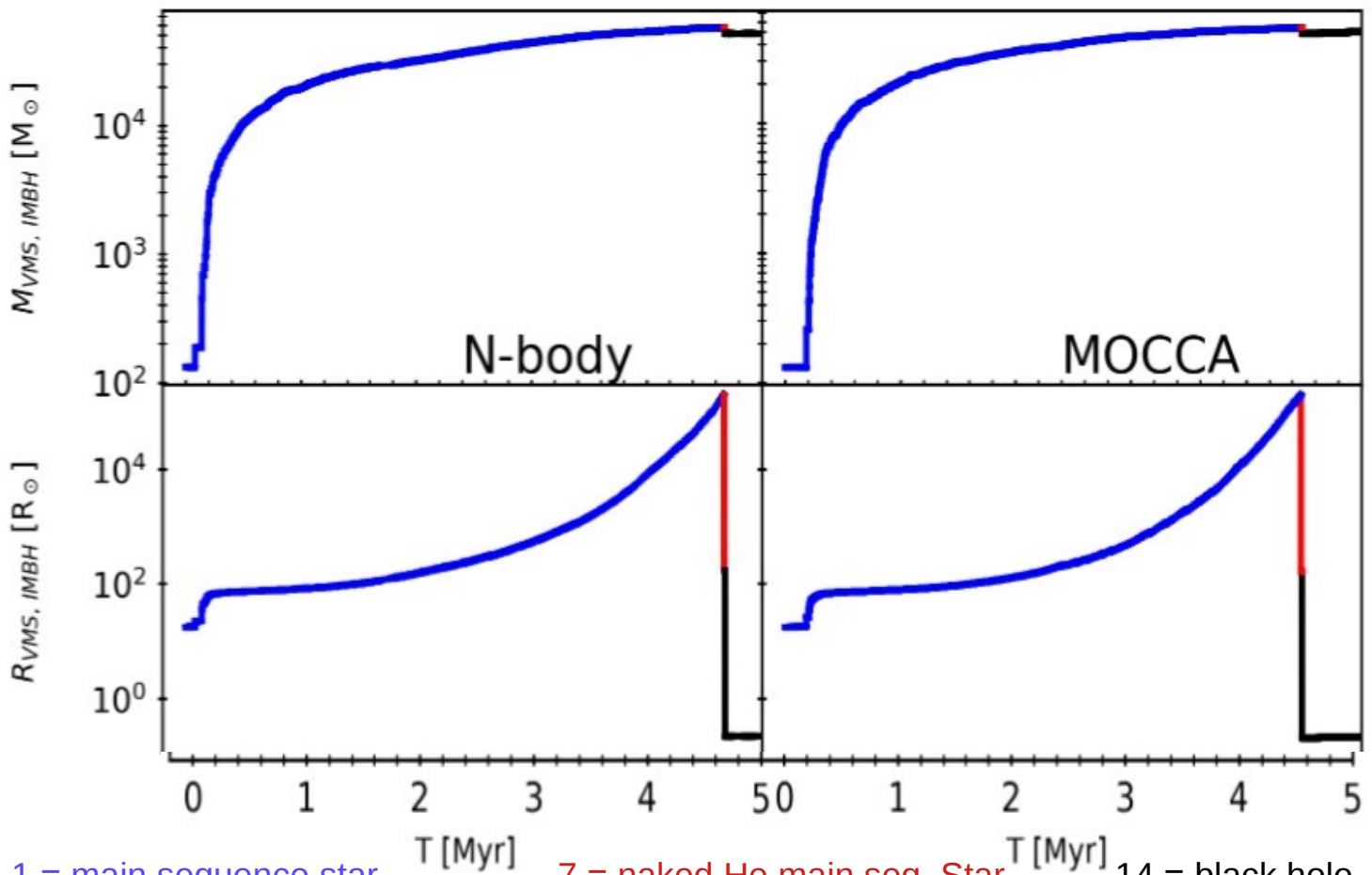

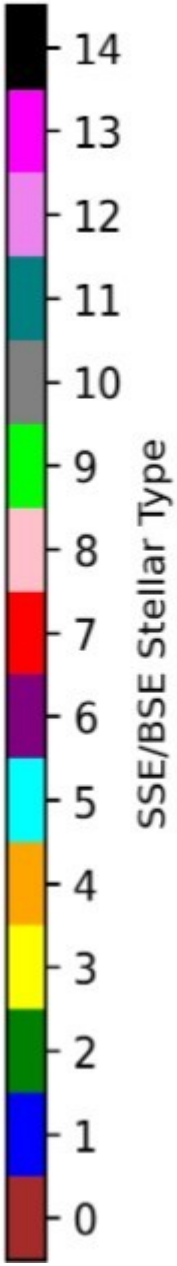

1 = main sequence star 7 = naked He main seq. Star 14 = black hole

Extended SSE/BSE stellar evolution, originally Hurley et al. 2002, 2005

1) Star Cluster Simulations/
   Black Holes/Grav. Waves
2) Nuclear Star Clusters
3) Code(s) and Hardware
4) Summary and References

Setting the stage: the galactic nucleus

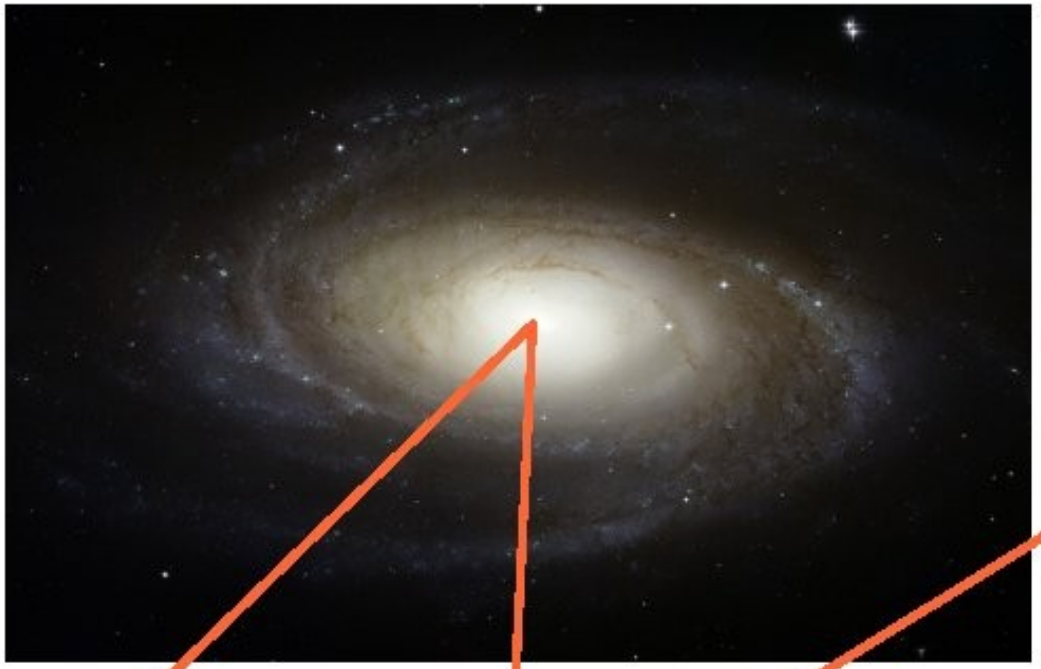

Size ~ 10 Kpc
Density ~ 0.05 M_{sun} pc^{-3}
Vel. Disp. ~ 40 Km/s
Relaxation time ~ 10^{15} yrs.

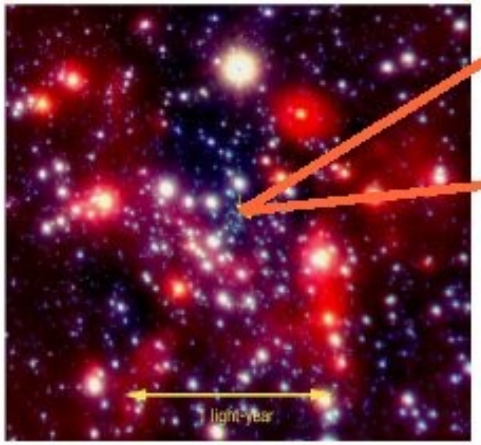

Size ~ 1-10 pc
Density ~ 10^{6-8} M_{sun} pc^{-3}
Vel. Disp. ~ 10^{2-3} Km/s
Relaxation time ~ 10^{8-9} yrs.

Size ~ 10^{-7}-10^{-4} pc
$Rs = 2G\,M_{BH}/c^2$
$R_t \sim (\alpha\, M_{BH}/m_*)^{1/3}\, R_*$
Loss cone aperture: θ

Slide: Miguel Preto

Distribution of stars

Model: Panamarev, Just, Spurzem, Berczik, Wang, Arca Sedda 2019, MNRAS
"DRAGON" of Galactic Center (one million bodies, SMBH, 1% hard binaries)

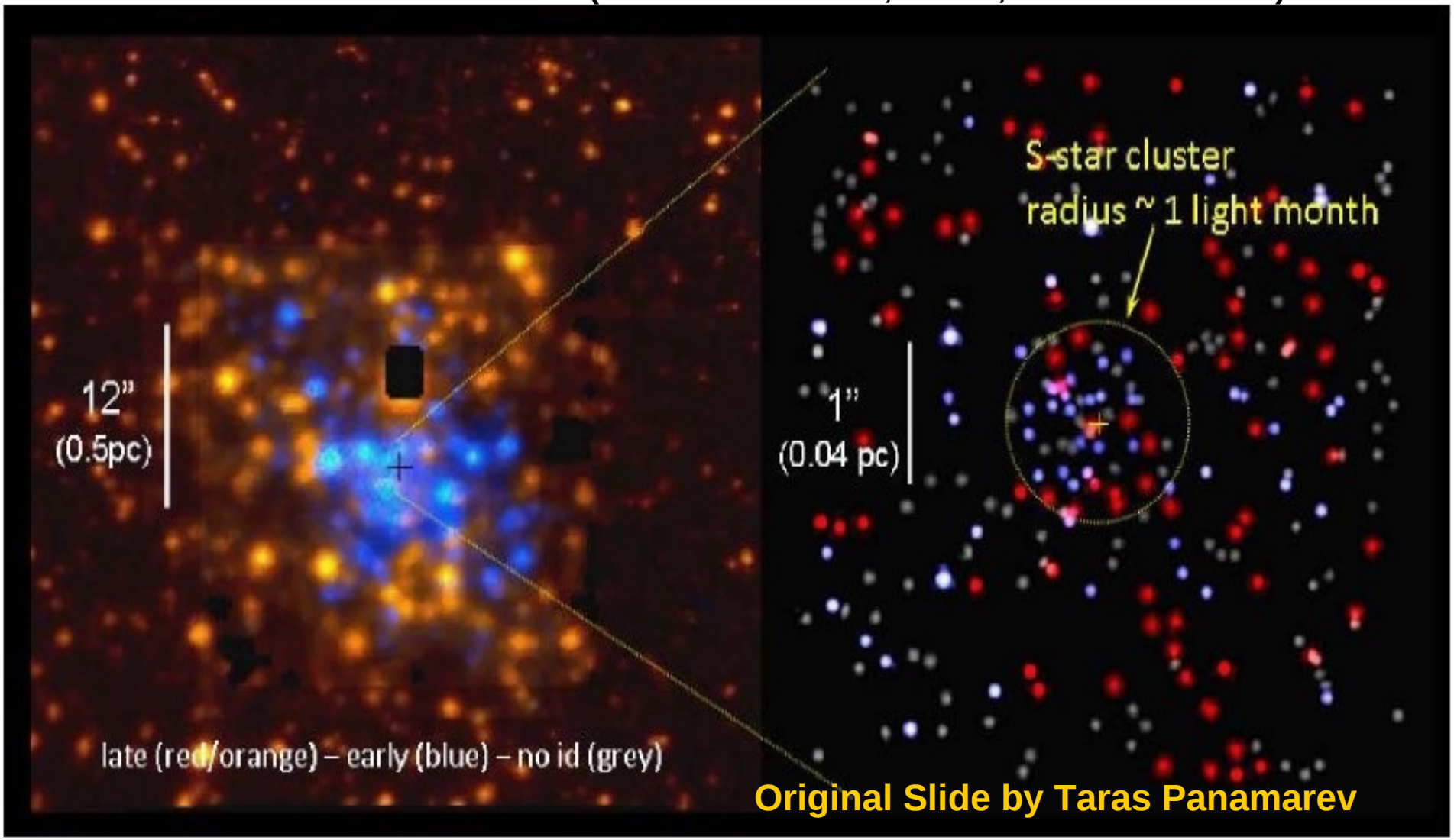

Original Slide by Taras Panamarev

Star Clusters around (supermassive) black holes

(From Frank & Rees 1976
See also:
Dokuchaev & Ozernoy 1977abc)

Predicted:
Char. Density profile
$n(r) \sim r^{-7/4}$

r_S : Schwarzschild – rad.
r_T : tidal disruption rad.
(solar type star)
r_{coll} : stellar collisions inside
r_h : grav. Influence rad.
r_{crit} : loss cone maximum
(spherical symmetry)
r_{max}: Oscillation in equipartition

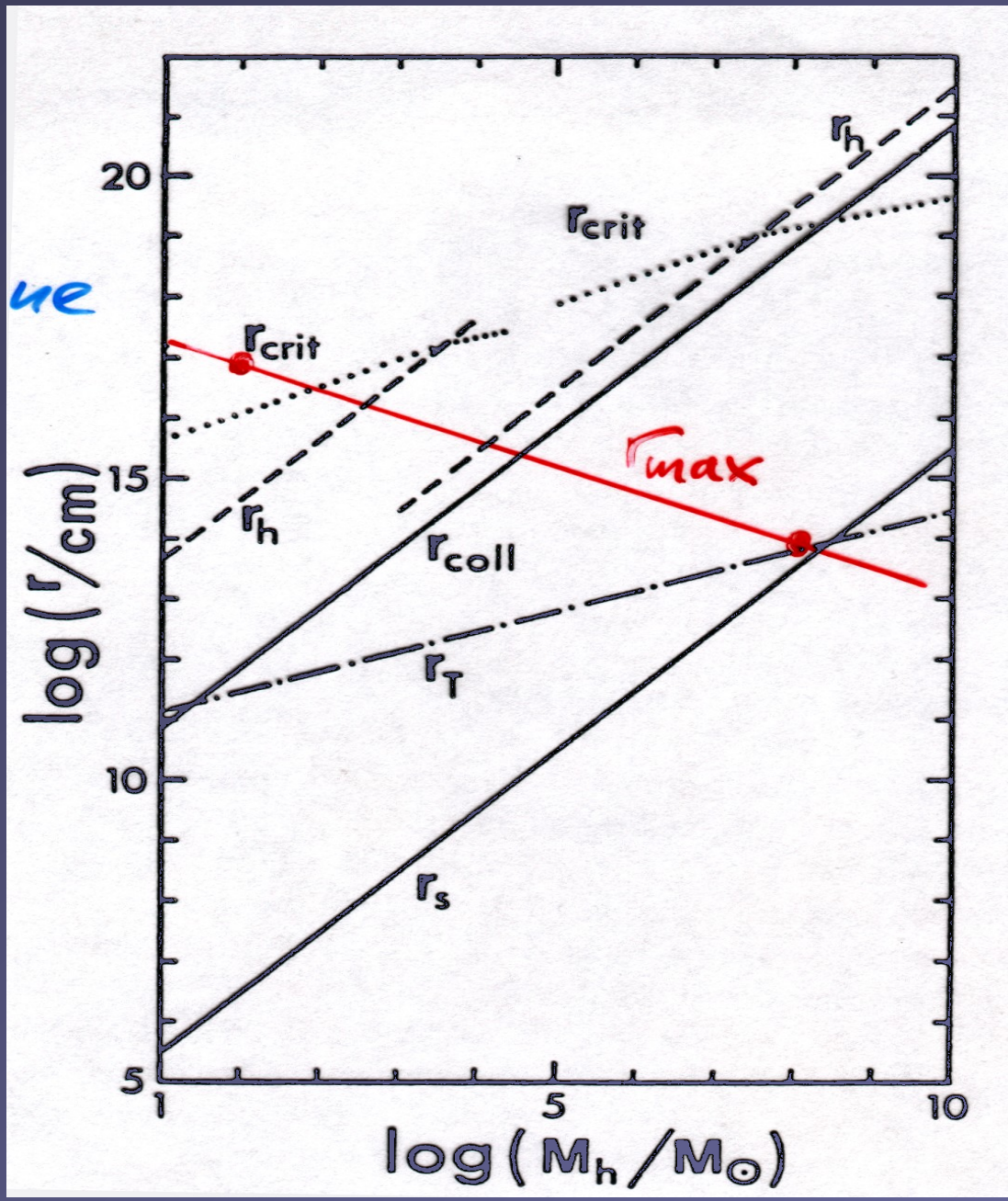

Mon. Not. R. Astron. Soc. **352,** 655–672 (2004) doi:10.1111/j.1365-2966.2004.07956.x

Accretion of stars on to a massive black hole: a realistic diffusion model and numerical studies

P. Amaro-Seoane,★ M. Freitag★ and R. Spurzem★
Astronomisches Rechen-Institut, Mönchhofstraße 12-14, Heidelberg, D-69120, Germany

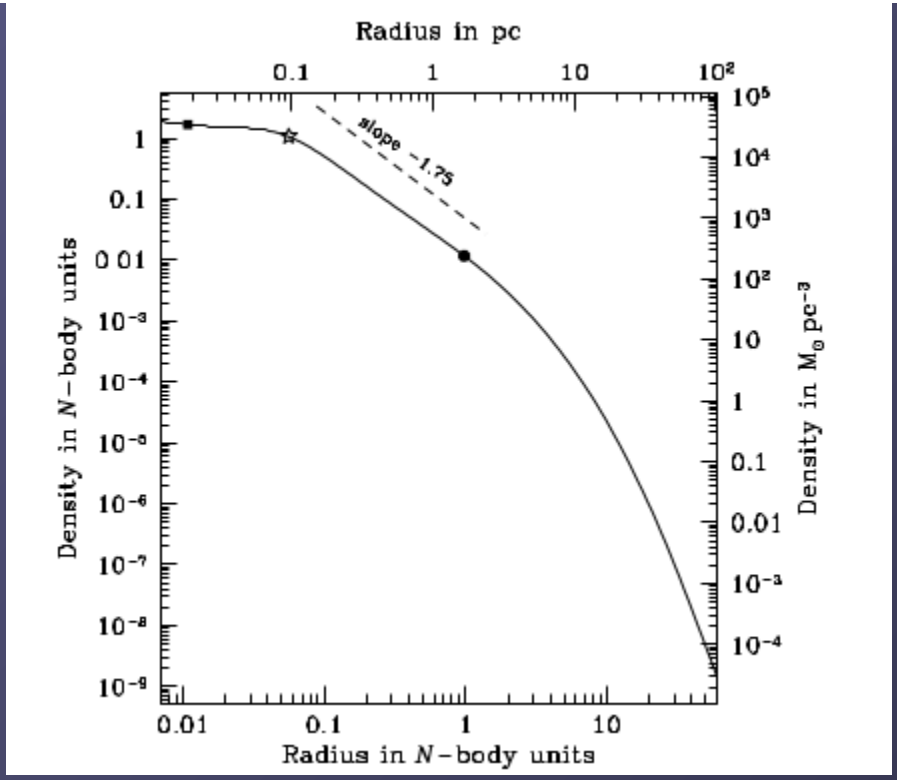

DRAGON Galactic Center Simulations

r_h : init / 5 Gyr

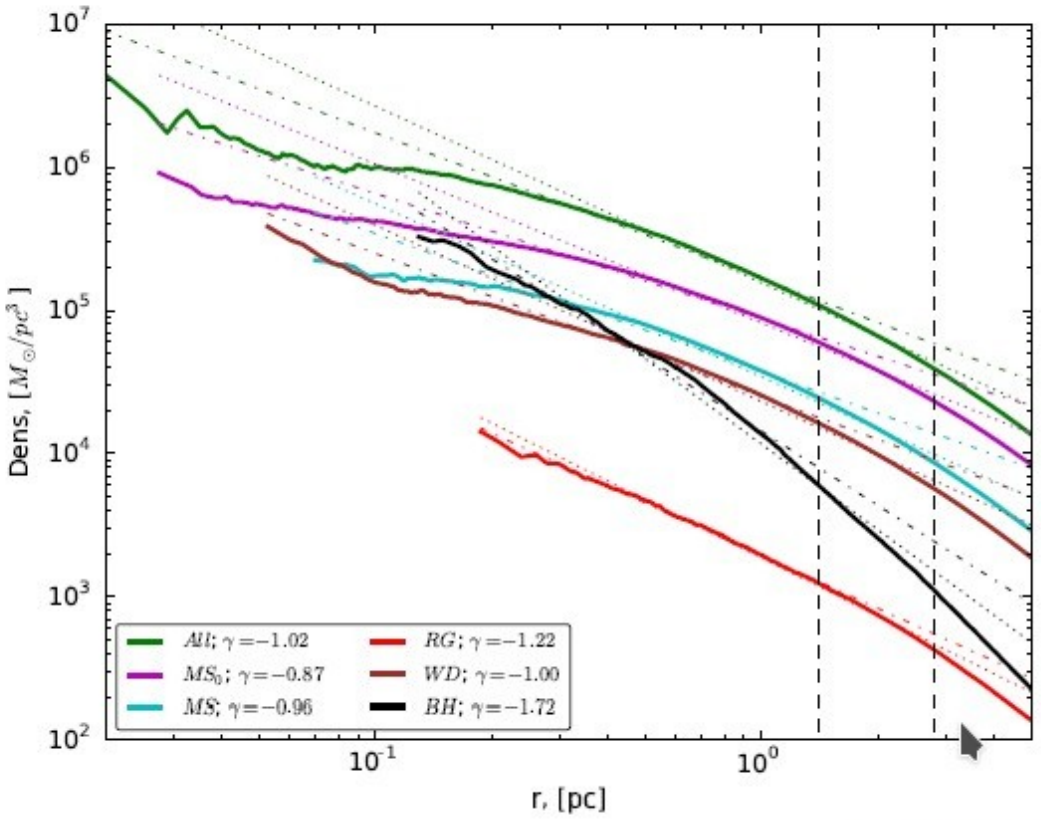

Initial Data:

1 million stars

10% fixed SMBH mass

Zero age pop, 0.8 – 100

Spherical

Density Profiles of stars and *-mass Black Holes in the Galactic Center after 5 Gyr

Extremely simple "accretion radius" For ALL objects.

FIGURE 4.3: Stellar density profiles at t = 5 Gyr for different stellar types. Thick solid lines correspond to: All - all stars, MS_{low} - low mass main sequence stars, MS - main sequence, RG - red giants, WD - white dwarfs, BH - black holes. Corresponding power-law slopes fitted inside the initial and final influence radii of the SMBH are shown as dash-dotted and dotted lines of the same colour. The dashed vertical lines denote the initial influence radius ($r = 1.4pc$) and the influence radius at $t = 5$Gyr ($r \sim 2.8pc$) of the SMBH. The power-law indices fitted inside $r = 1.4pc$ are shown in the legend.

Panamarev, Just, Spurzem, et al. 2019

Panamarev, …, Just, Spurzem, 2018, MNRAS

DRAGON Galactic Center Simulations

TABLE 4.1: Properties of different stellar types at $t = 5$ Gyr.

Stellar type	N_{tot}	$<m>$ $(M_\odot)$	$\gamma(r < 1.4pc)$	$\gamma(r < 2.8pc)$	$\dot{N}_{acc}$ (Gyr^{-1})	$\dot{N}_{acc}(r < 3$ (Gyr^{-1})
Low-mass main sequence	5.0×10^7	0.25	-0.87 ± 0.01	-1.11 ± 0.03	3278	-
Main sequence	4.3×10^6	0.92	-0.96 ± 0.02	-1.21 ± 0.05	658	-
Red giant	1.5×10^5	1.24	-1.22 ± 0.12	-1.34 ± 0.15	39	-
White dwarf	1.6×10^6	0.71	-1.00 ± 0.02	-1.23 ± 0.03	138	225
Black hole	1.8×10^4	10.05	-1.72 ± 0.04	-1.98 ± 0.07	2	3
All stars	5.8×10^7	0.33	-1.02 ± 0.02	-1.23 ± 0.03	4120	-

Panamarev, Just, Spurzem, et al. MNRAS, 2019

Panamarev, Berczik,…, Just, Spurzem, 2018, MNRAS

First Simulation of its kind – BUT!!

- **One single accretion (“tidal”) radius for ALL objects!**
- **Rather outdated stellar evolution (winds/remnants/BH mergers)**
- **Neutron stars / pulsars lost (no gal. Potential, too high kicks)**

Tidal Disruption Events for DRAGON-III

(5 Improvements)

Tidal Disruption of a star by a SMBH

Standard Picture

Rees (1988)

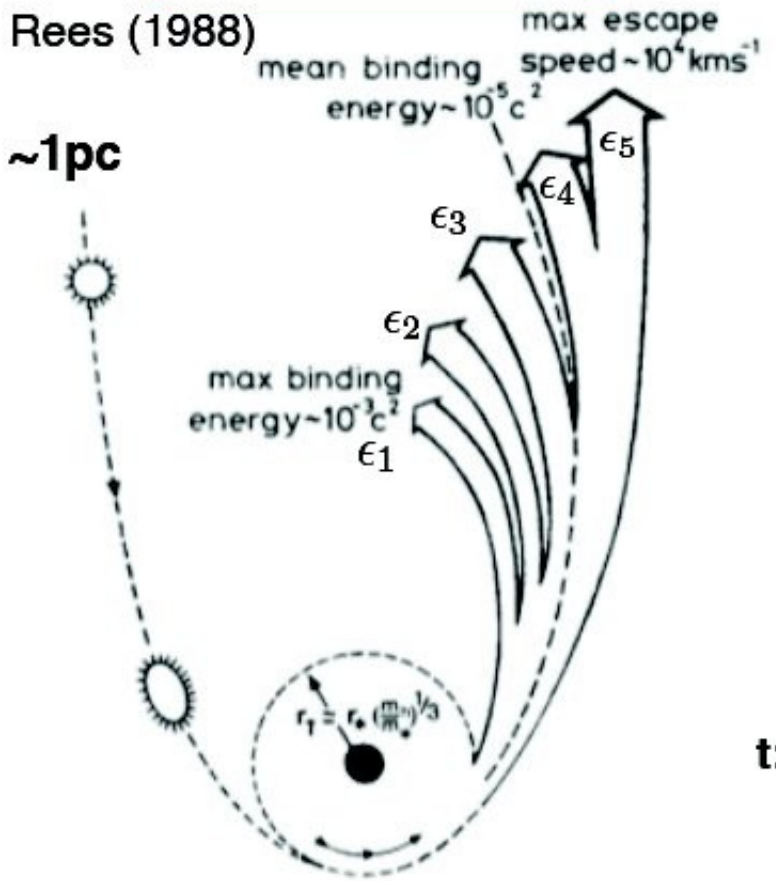

Tidal disruption radius
(Tidal force=self-gravity force):

$$r_{\rm t} = \left(\frac{M_{\rm BH}}{m_*}\right)^{1/3} r_*$$

Δε: Spread in debris energy by tidal force

$$\Delta\epsilon = \frac{GM_{\rm BH}}{r_{\rm t}}\frac{r_*}{r_{\rm t}}$$

ε: Debris specific energy

if ε>=0	Stellar debris flies away from the black hole
if ε< 0	Stellar debris is bounded by the black hole's gravity and falls back to black hole

t: Fallback time for most tightly bound debris

$$t_{\rm fall} \sim 0.1\,{\rm yr}\left(\frac{r_*}{R_\odot}\right)^{3/2}\left(\frac{m_*}{M_\odot}\right)^{-1}\left(\frac{M_{\rm BH}}{10^6 M_\odot}\right)^{1/2}$$

What is the rate of mass fallback?

Slide by Kimitake Hayasaki

Mass fallback rate I.

$$\frac{dM}{dt} = \frac{dM(\epsilon)}{d\epsilon}\left|\frac{d\epsilon}{dt}\right| \quad (\epsilon < 0)$$

Specific energy: $\epsilon \approx -\frac{GM_{\rm BH}}{2a}$

Its time derivative:

$$\frac{d\epsilon}{dt} = -\frac{1}{3}(2\pi G M_{\rm BH})^{2/3} t^{-5/3}$$

(by using Keplerian third law)

$$\frac{dM}{dt} \propto t^{-5/3}$$

Rees's conjecture (1988)

Differential mass-energy distribution of stellar debris

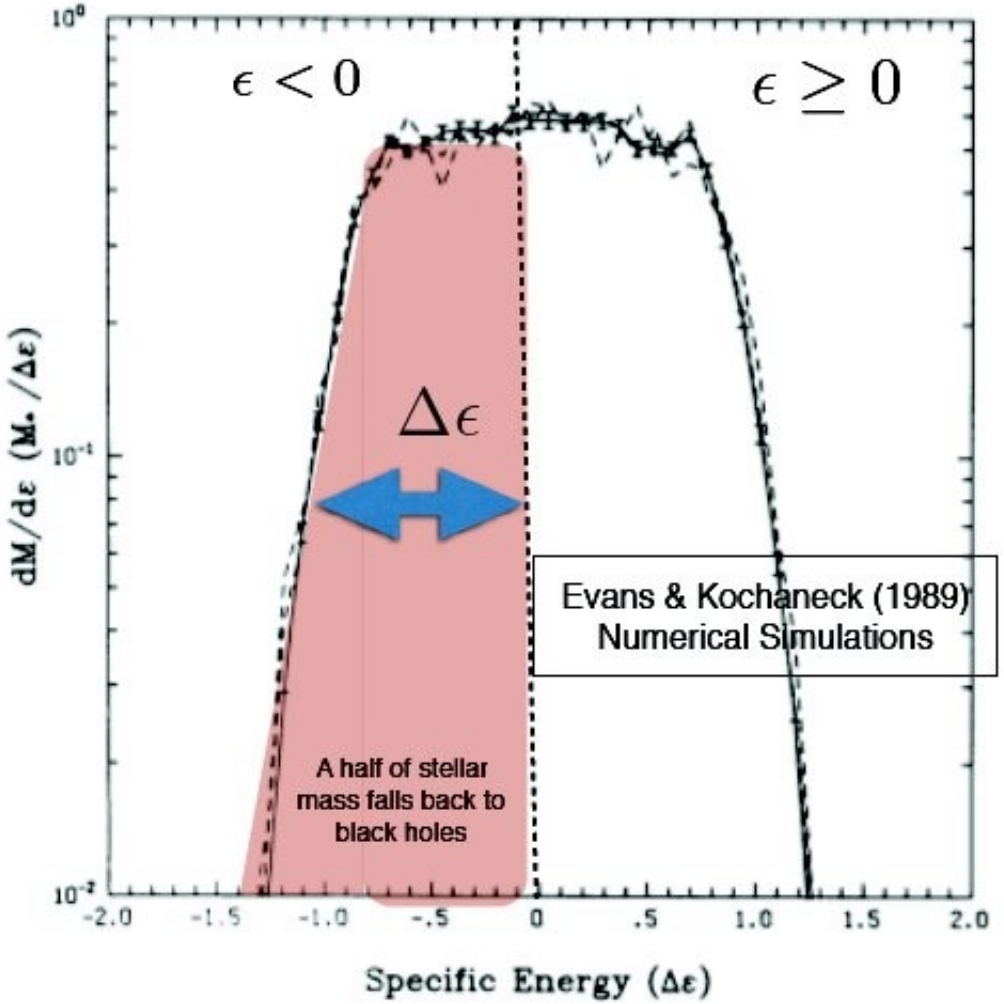

Slide by Kimitake Hayasaki

DRAGON III of Galactic Center

tidal disruption and partial accretion – improvement 1

(Cho Master Thesis 2024, in preparation for Cho et al. 2025, A&A;

see also Zhong, Li, Berczik, Sp. 2022, Hayasaki, Zhong, Hayasaki, Li, Berczik, Sp. 2023)

Classification

For eccentric orbits, if $\Delta\epsilon + \epsilon_{orb} \leq 0$, all the stellar debris are bound by the black hole after TDE.

$$e_{crit,1} = 1 - \frac{2}{\beta}\left(\frac{m_\star}{M_{BH}}\right)^{1/3}$$

For a hyperbolic orbit , if $-\Delta\epsilon + \epsilon_{orb} \leq 0$,

$$e_{crit,2} = 1 + \frac{2}{\beta}\left(\frac{m_\star}{M_{BH}}\right)^{1/3},$$

above which all the stellar debris should escape from BH.

(Hayasaki et al, 2018)

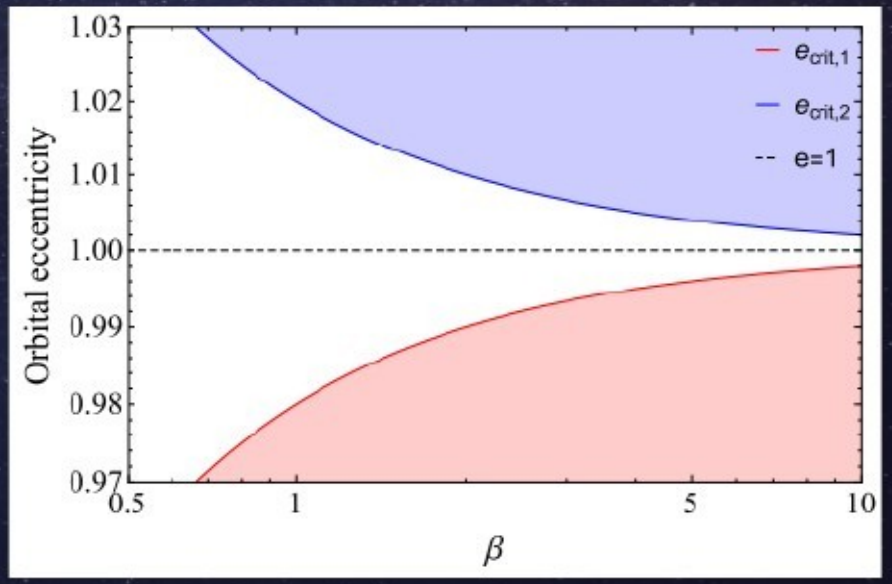

Hayasaki et al, 2018

Results – TDE (Slide by Philip Cho, Pilot Simulations)

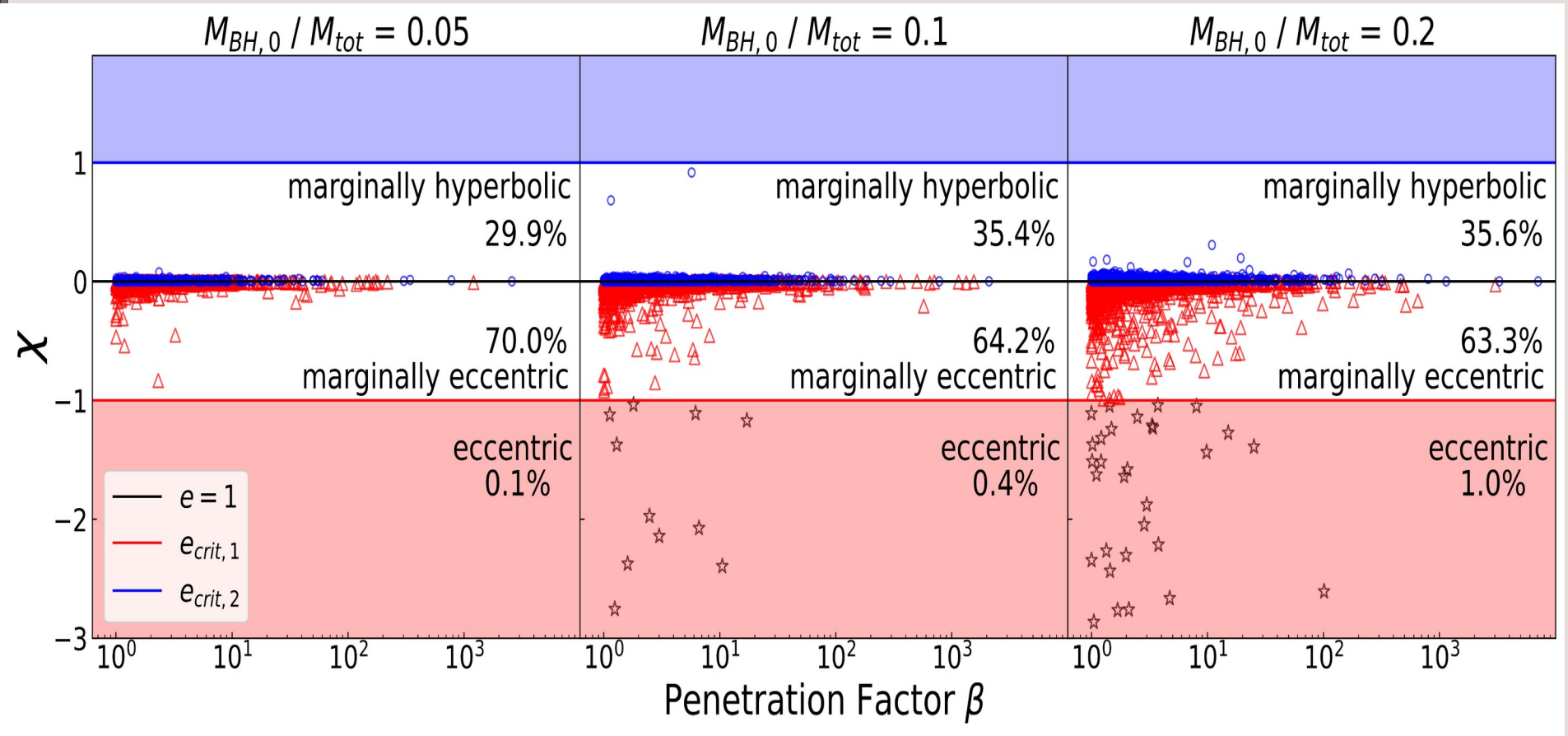

$ß = r_t / r_p$; $\chi = (e-1)/\Delta e$; $\Delta e = (2/ß)(m_*/M_{BH})^{(1/3)}$

DRAGON III of Galactic Center

tidal disruption and partial accretion – Improvement 1 (Cho)

Mass Fraction of a tidally disrupted star accreted to SMBH

Using first order analytic model of energy profile in star (top-hat)

(see Hayasaki et al. 2013, 2018)

Eccentric TDE **Hyperbolic TDE**

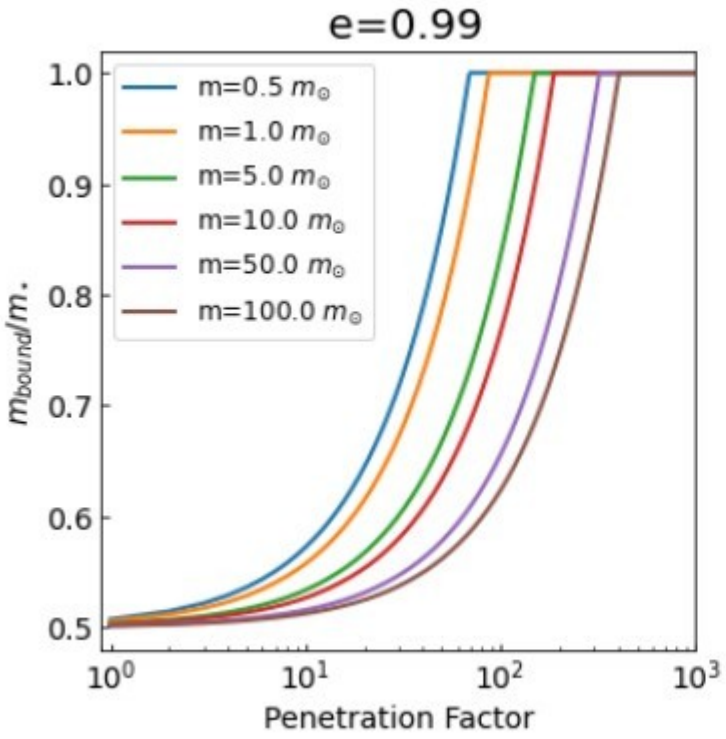

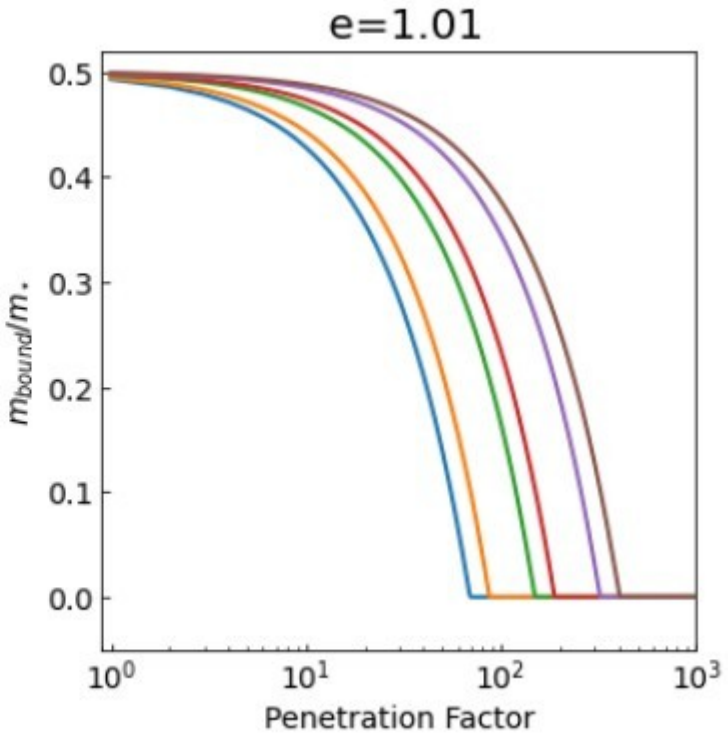

DRAGON III of Galactic Center

tidal disruption and partial accretion – improvement 3 (Cho)

Preliminary Results: Percentage of Ecc./Hyp. Partial TDEs

(Relevant for TDE light curves)

Taken from

Philip Seunghee Cho:

Master Thesis

Univ. Heidelberg

2023

Model	CMBH	r_{acc}	N_{TDE}	M_{acc}	M_{esc}	f_e	f_{me}	f_p	f_{mh}	f_h
1		10^{-5}	245	$235M_\odot$	$107M_\odot$	2.1	86.5	0	11.4	0
2	$3792M_\odot$	10^{-4}	1210	$1051M_\odot$	$494M_\odot$	2.7	67.7	0	29.6	0
3		10^{-3}	3742	$2381M_\odot$	$1382M_\odot$	2.1	52.3	0	45.6	0
4		10^{-5}	597	$346M_\odot$	$250M_\odot$	0.5	88.1	0	11.4	0
5	$7583M_\odot$	10^{-4}	2842	$1784M_\odot$	$1191M_\odot$	1.3	63.4	0	35.3	0
6		10^{-3}	6963	$2883M_\odot$	$2138M_\odot$	1.96	50.6	0	47.4	0.04
7		10^{-5}	887	$306M_\odot$	$273M_\odot$	0.6	82.2	0	17.2	0
8	$15168M_\odot$	10^{-4}	4114	$1584M_\odot$	$1307\ M_\odot$	1.2	63.2	0	35.6	0
9		10^{-3}	9395	$3248M_\odot$	$2568\ M_\odot$	3.05	51.7	0	45.2	0.05

TABLE 3.1: Simulation Results. The model number is shown in the first column. The second and third column are the initial mass of CMBH, in solar mass unit, and the accretion radius in NB unit, respectively. The fourth column shows the total number of TDEs occurred. The fifth column shows the total accreted mass by the black hole, and the sixth column shows the total debris mass that escaped from the CMBH potential. From seventh to last columns, the percentage of each type of TDEs are shown.

DRAGON III of Galactic Center

Why is it important to know about TDE event rates from simulations?

Hundreds if not tens of thousands will be detected soon

(LSST, ZTF, ULTRASAT, eROSITA, …., Szekerzczes, Ryu et al. 2024, A&A)

We need to know about parameters of host galaxies, nuclear clusters

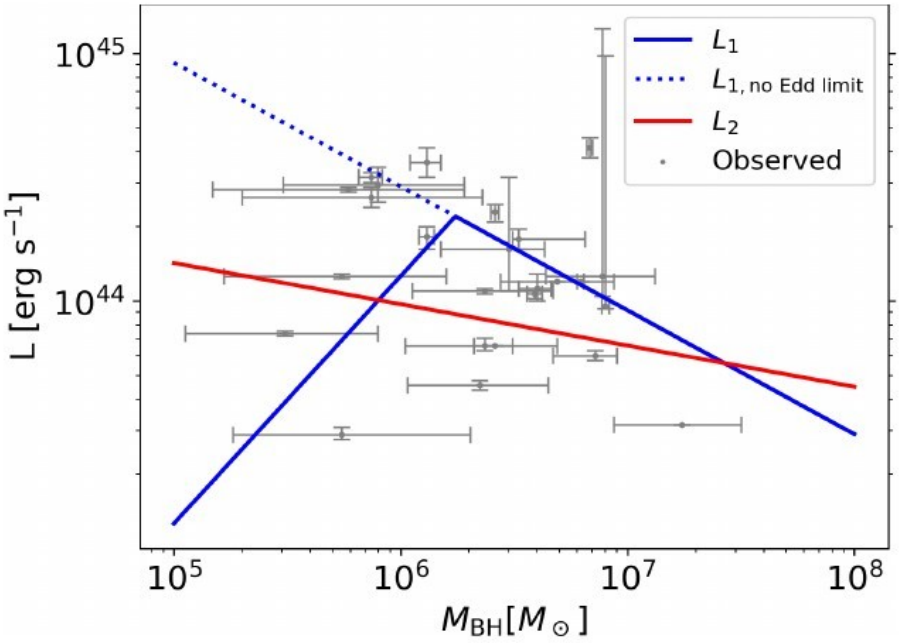

Fig. 2. Two luminosities of TDEs, L_1 (Eq. (6), Thomsen et al. 2022) and L_2 (Eq. (7), Ryu et al. 2020b) as a function of $M_{\rm BH}$ overlaid with observed optical TDEs using gray dots and error bars (see Table A.1 in Wong et al. 2022 and Table 1 in Ryu et al. 2020b, and references therein). The dotted blue line conveys L_1 as given by Eq. (6), whereas the solid blue line show the Eddington limited L_1.

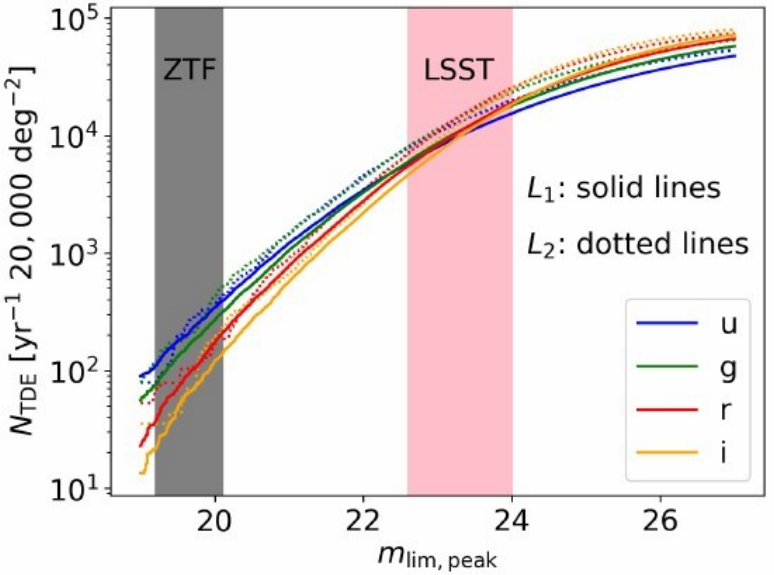

Fig. 6. Annual unlensed TDE detection rates as a function of the peak brightness, $m_{\rm lim,peak}$, at $T = 2 \times 10^4$ K for L_1 in solid lines and for L_2 shown in dotted lines. The limiting magnitudes for the different filters of ZTF and LSST surveys are within the gray and pink shaded areas, respectively. These limiting magnitudes are 0.7 brighter than the survey limiting magnitude $m_{\rm lim,survey}$ (i.e., $m_{\rm lim,peak} = m_{\rm lim,survey} - 0.7$), denoted by LSST1, in order for TDEs to have multiple detections near their peak brightness above the limit $m_{\rm lim,survey}$.

DRAGON III of Galactic Center

accretion and disruption processes depend on type of object – improvement 2

(Minzburg Master Thesis to be published)

Improvement 2: Tidal Disruption Radius varies with * parameters (m,r);

Include relativistic inspirals of bh and ns (not plotted here)

Include direct capture of very low mass ms stars (not plotted here)

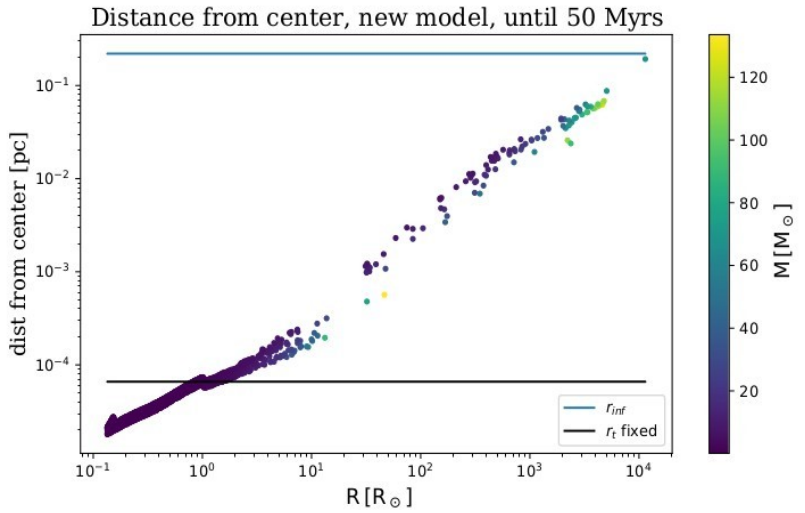

Figure 3.13: Distances of accreted objects vs their size in $R_\odot$ colorcoded in ma time until 50 Myrs. Accreted stars have sizes between 0.1 and 1(most massive star has ~ $130M_\odot$. The distances span 4 orders of r between 10^{-5} and 10^{-1} pc.

black hole mass growth

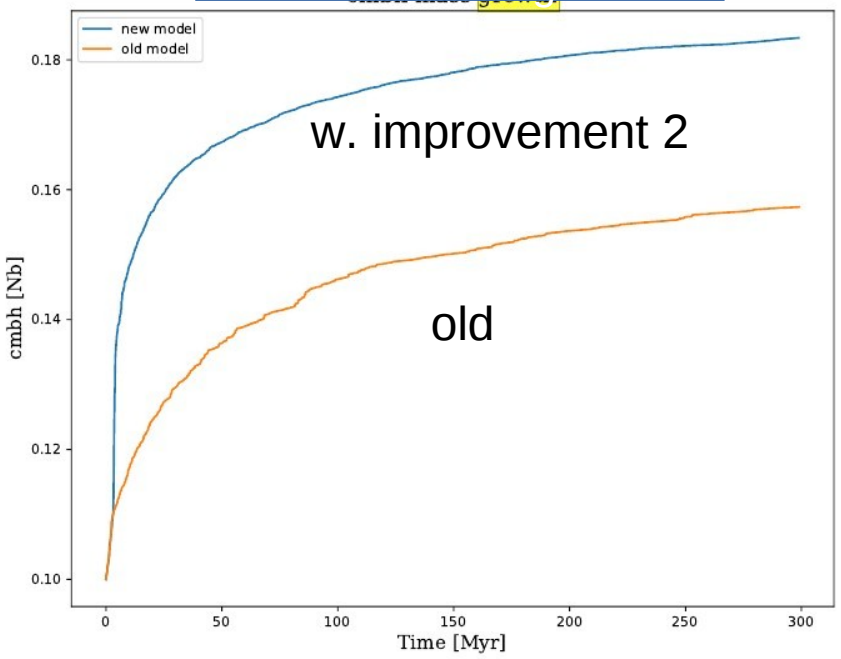

Figure 3.15: Mass growth of the central massive black hole throughout the simulation for the old model (orange) and new model (blue). While a steeper rise at the beginning of the simulation can be observed for the new model, the slopes appear similar for both models after 100 Myrs.

Improvement 3:
Partial and Full Tidal Disruption Events in Nuclear Star Cluster Simulations

From: Zhong, Li, Berczik, Spurzem, 2022, ApJ

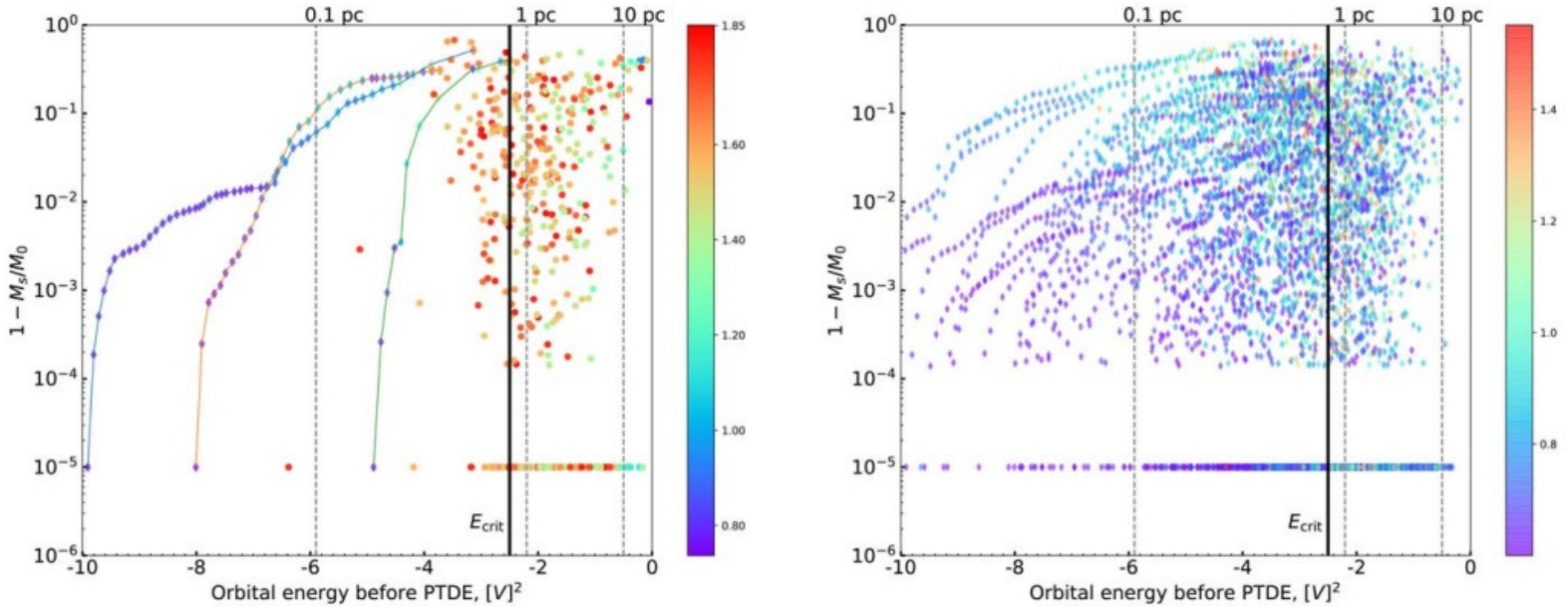

Figure 4. Distribution of stars that produce PTDEs in the parameter space spanned by the mass (m_s) and specific orbital energy (E_{tot}) of the stars. For every PTDE, the values of m_s and E_{tot} are measured at the moment immediately before the onset of the event. Colors indicate the penetration factor β. The vertical solid line marks the position of the critical energy, and the corresponding physical radius is roughly 0.7 pc. For clarity, the vertical axis shows the quantity $1 - m_s/m_0$, where $m_0 = 1/N$ [M] is the initial mass of the star, and is set to log scale. However, with this configuration, the PTDEs produced by the normal stars are not visible in the figure because $1 - m_s/m_0 = 0$. We have artificially reset the value of $1 - m_s/m_0$ to 10^{-5} for the PTDEs produced by normal stars. The left panel shows the PTDEs after which the leftover stars are ejected, while the right panel shows the PTDEs after which the leftover stars are retained in the star cluster. In the left panel, we also plot the historical PTDEs (diamonds connected by lines) for three individual stars. This figure is generated from the data of one realization of the fiducial model.

More PTDE than FTDE – orbits diverse!

Full and Partial Tidal Disruption Events (FTDE / PTDE)

TD Scheme

Improvement 4

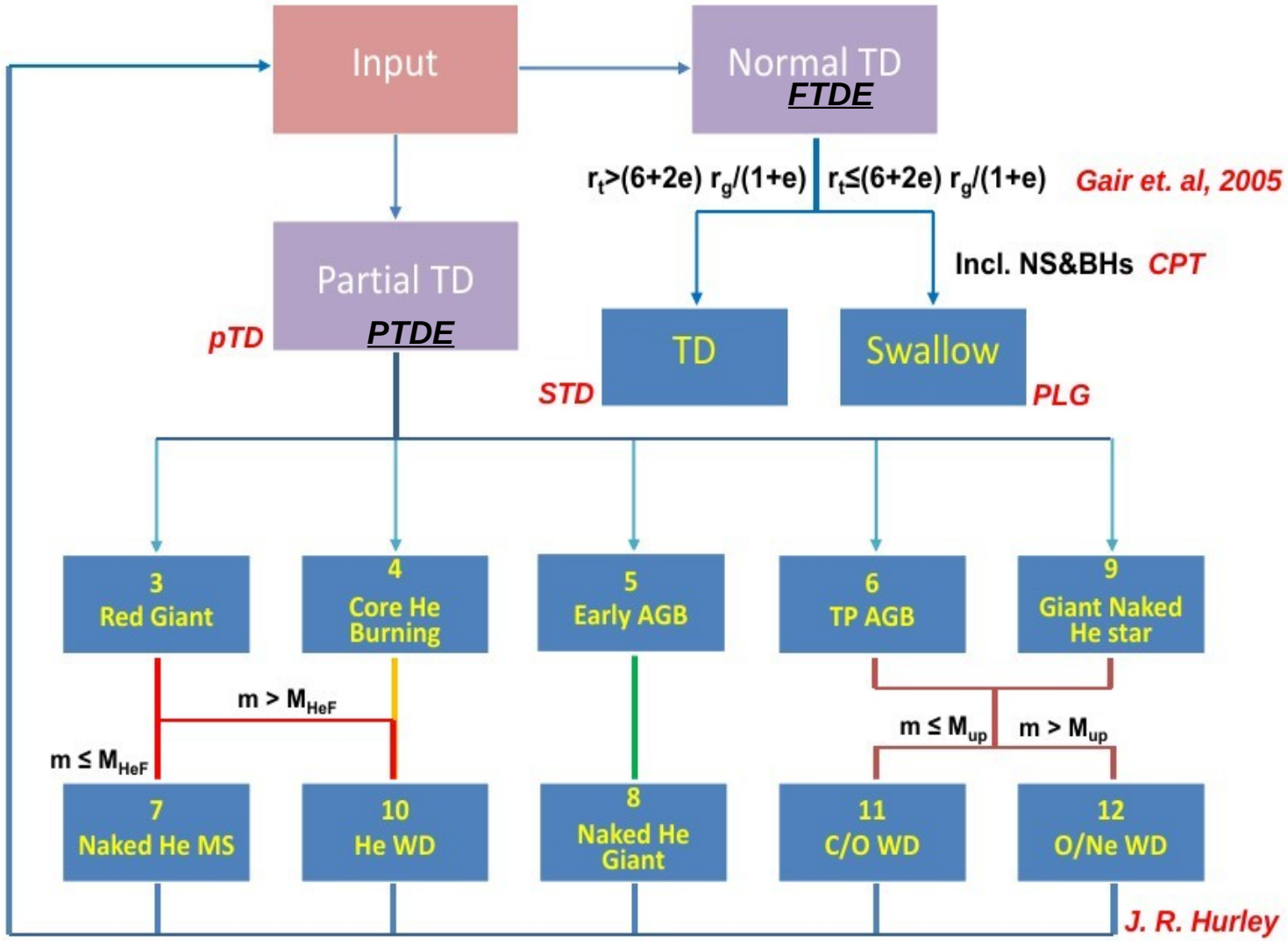

Li, Zhong, Berczik, Spurzem, Chen, Liu, MNRAS 2023

Tidal Disruption Events in Merging Nuclear star clusters

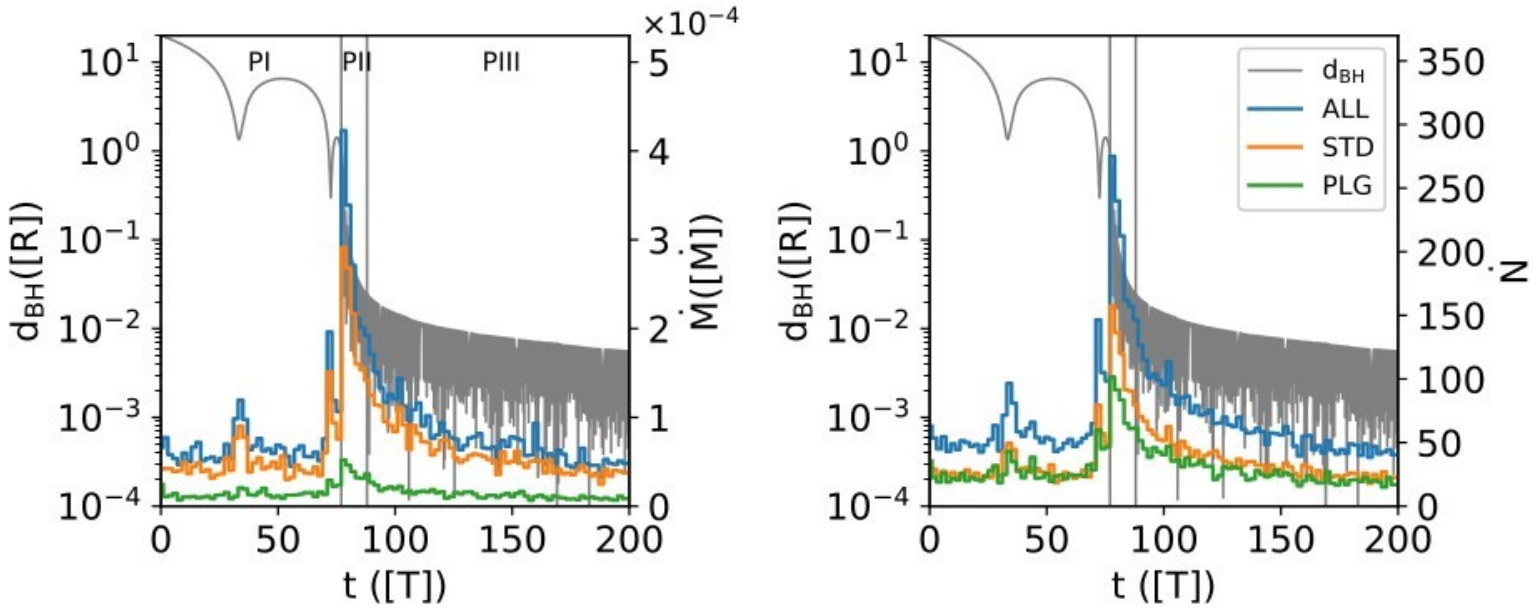

Figure 6. The tidal disruption/swallow evolution of MS stars. The left panel and right panel are, respectively, the evolution of the mass accretion rate and the event rate. The blue, orange, and green solid lines represent the results of all of MS stars, standard TDEs, and MS stars which directly plunge into the SMBH, respectively. The two vertical gray lines divide the evolution into three phases.

Li, Zhong, Berczik, Spurzem, Chen, Liu, MNRAS 2023

DRAFT VERSION DECEMBER 20, 2024
Typeset using LaTeX **twocolumn** style in AASTeX631

Formation and Evolution of Compact Binaries Containing Intermediate Mass Black Holes in Dense Star Clusters

SEUNGJAE LEE [1], HYUNG MOK LEE [2,3], JI-HOON KIM [1,3,4], RAINER SPURZEM [5,6,7], JONGSUK HONG [8], AND EUNWOO CHUNG [1]

[1] *Center for Theoretical Physics, Department of Physics and Astronomy, Seoul National University, Seoul 08826, Korea*
[2] *Research Institute for Basic Sciences, Seoul National University, Seoul 08826, Korea*
[3] *Seoul National University Astronomy Research Center, Seoul 08826, Korea*
[4] *Institute for Data Innovation in Science, Soul National University, Seoul 08826, Korea*
[5] *Astronomisches Rechen-Institut, Zentrum für Astronomie der Universität Heidelberg, Mönchhofstr. 12-14, D-69120 Heidelberg, Germany*
[6] *National Astronomical Observatories and Key Laboratory of Computational Astrophysics, Chinese Academy of Sciences, 20A Datun Rd., Chaoyang District, Beijing 100101, China*
[7] *Kavli Institute for Astronomy and Astrophysics, Peking University, Yiheyuan Lu 5, Haidian Qu, 100871, Beijing, China*
tronomy and Space Science Institute, Daejeon 34055, Republic of Korea

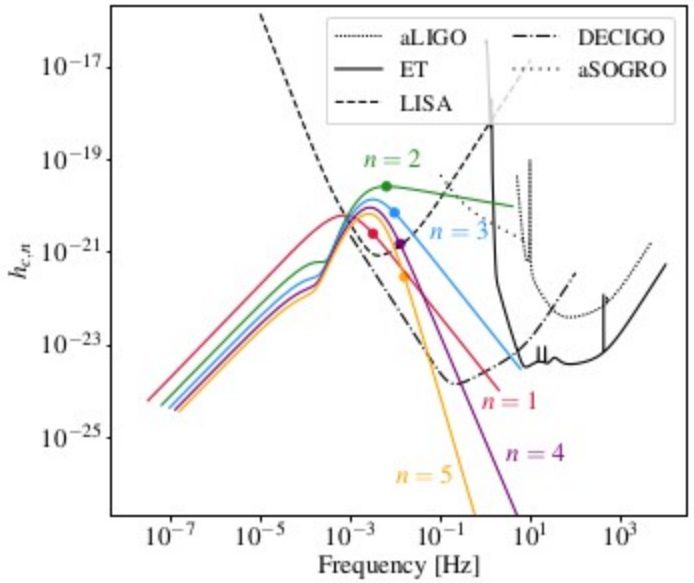

Figure 2. A sample illustration of the characteristic amplitude of the n-th harmonics, $h_{c,n}$, from $n = 1$ to 5 emitted during the IMRI. The *dashed black V-shaped curve* represents LISA's sensitivity curve ($\sqrt{fS_h(f)}$; see Section 2.2). while two *U-shaped curves* indicate the sensitivities of aLIGO (*densely-dotted line*) and ET (*solid line*).

TDE in Nbody6++GPU - Improvement 5

https://arxiv.org/abs/2503.22109

1) Star Cluster Simulations/
   Black Holes/Grav. Waves
2) Nuclear Star Clusters
3) Code(s) and Hardware
4) Summary and References

Code(s)

Nbody6++GPU

Physical and Numerical Methods: Direct Simulations
Direct: high accuracy / active-inactive particles

The Hermite Scheme: 4th Order on two time points

$$\vec{a}_0 = \sum_j G m_j \frac{\vec{R}_j}{R_j^3} \quad ; \quad \dot{\vec{a}}_0 = \sum_j G m_j \left[\frac{\vec{V}_j}{R_j^3} - \frac{3(\vec{V}_j \cdot \vec{R}_j)\vec{R}_j}{R_j^5} \right] ,$$

$$\vec{x}_p(t) = \frac{1}{6}(t - t_0)^3 \dot{\vec{a}}_0 + \frac{1}{2}(t - t_0)^2 \vec{a}_0 + (t - t_0)\vec{v} + \vec{x} ,$$

$$\vec{v}_p(t) = \frac{1}{2}(t - t_0)^2 \dot{\vec{a}}_0 + (t - t_0)\vec{a}_0 + \vec{v} ,$$

Repeat Step 1 at t_1 using predicted x,v → a_1, $\mathring{a}_1$

NBODY6++GPU: https://github.com/nbody6ppgpu/

Physical and Numerical Methods: Direct Simulations

$$\frac{1}{2}\vec{a}^{(2)} = -3\frac{\vec{a}_0 - \vec{a}_1}{(t-t_0)^2} - \frac{2\vec{\dot{a}}_0 + \vec{\dot{a}}_1}{(t-t_0)}$$

$$\frac{1}{6}\vec{a}^{(3)} = 2\frac{\vec{a}_0 - \vec{a}_1}{(t-t_0)^3} - \frac{\vec{\dot{a}}_0 + \vec{\dot{a}}_1}{(t-t_0)^2} \ ,$$

The Hermite Step

Get Higher Derivatives

$$\vec{x}(t) = \vec{x}_p(t) + \frac{1}{24}(t-t_0)^4\vec{a}_0^{(2)} + \frac{1}{120}(t-t_0)^5\vec{a}^{(3)} \ ,$$

$$\vec{v}(t) = \vec{v}_p(t) + \frac{1}{6}(t-t_0)^3\vec{a}_0^{(2)} + \frac{1}{24}(t-t_0)^4\vec{a}_0^{(3)} \ .$$

The Corrector Step – this is not time symmetric!

Physical and Numerical Methods: Direct Simulations

P(EC)^n Scheme, n=1, Kokubo et al. 1998, Hut et al. 1995

$$\boldsymbol{x}_{\mathrm{p},j} = \boldsymbol{x}_j + \boldsymbol{v}_j(t - t_j) + \frac{\boldsymbol{a}_j}{2}(t - t_j)^2 + \frac{\dot{\boldsymbol{a}}_j}{6}(t - t_j)^3,$$

$$\boldsymbol{v}_{\mathrm{p},j} = \boldsymbol{v}_j + \boldsymbol{a}_j(t - t_j) + \frac{\dot{\boldsymbol{a}}_j}{2}(t - t_j)^2,$$

1 higher order in x-prediction

$$\boldsymbol{x}_1 = \boldsymbol{x}_0 + \frac{1}{2}(\boldsymbol{v}_1 + \boldsymbol{v}_0)\Delta t - \frac{1}{10}(\boldsymbol{a}_1 - \boldsymbol{a}_0)\Delta t^2 + \frac{1}{120}(\dot{\boldsymbol{a}}_1 + \dot{\boldsymbol{a}}_0)\Delta t^3$$

$$\boldsymbol{v}_1 = \boldsymbol{v}_0 + \frac{1}{2}(\boldsymbol{a}_1 + \boldsymbol{a}_0)\Delta t - \frac{1}{12}(\dot{\boldsymbol{a}}_1 - \dot{\boldsymbol{a}}_0)\Delta t^2.$$

This is time-symmetric (exchange 0,1, change sign(v),sign(å))!
(But pred/corr diff. in x,v of field particles neglected)

By iteration n>1 it improves further.

Physical and Numerical Methods: Direct Simulations

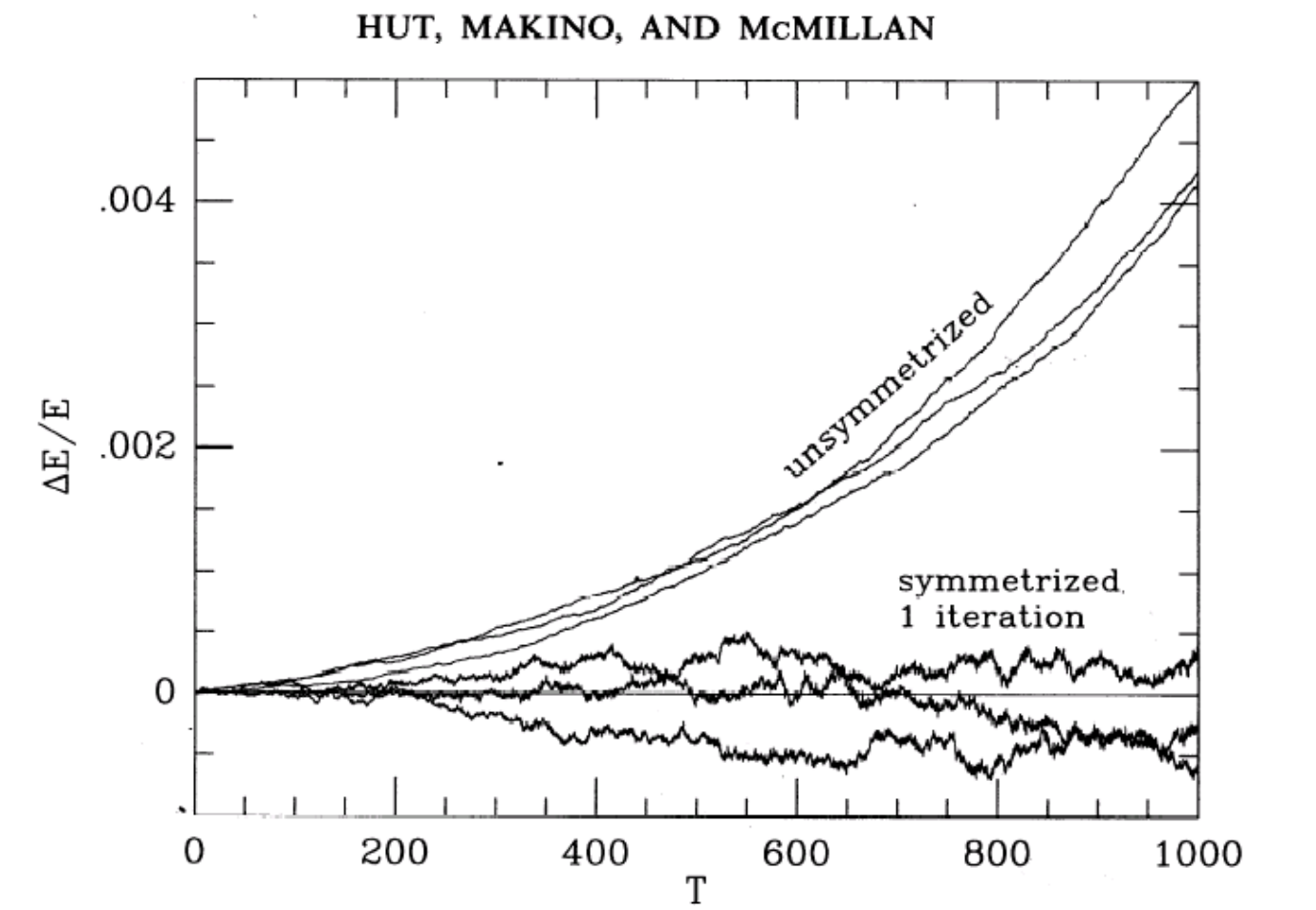

1995

N=100

1000 orb.times

Physical and Numerical Methods: Direct Simulations

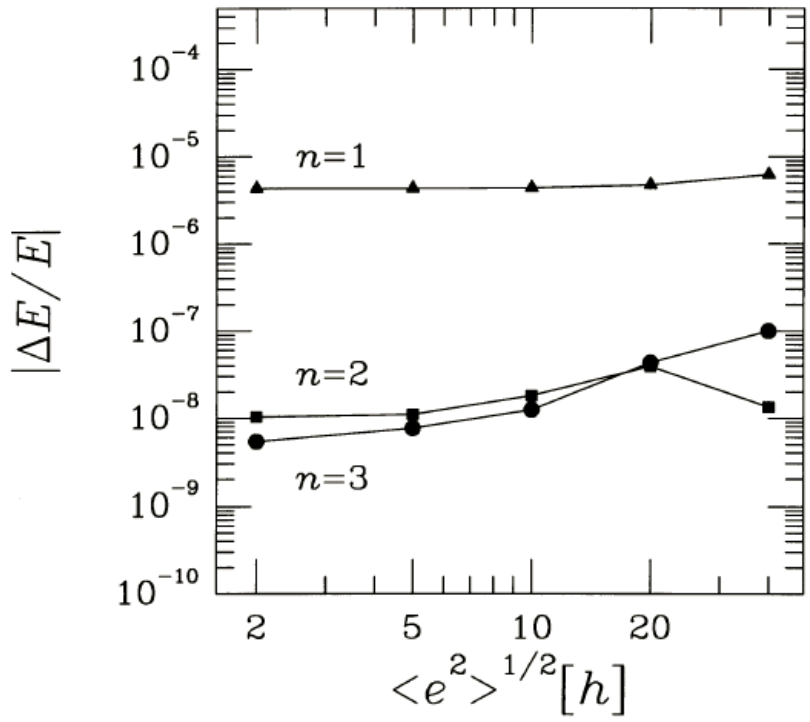

Figure 4. The relative error of the total energy of a planetesimal system that consists of 100 equal-mass ($m = 10^{25}$ g) bodies after $1000T_K$ as a function of the initial $\langle e^2 \rangle^{1/2}$ for the P(EC)^n ($n = 1, 2, 3$) Hermite schemes with the hierarchical time-step scheme. The triangles show the result of the $n = 1$ scheme, the squares $n = 2$ and the circles $n = 3$.

Kokubo et al. 1998

Yoshinaga et al. 1999

Kokubo & Makino 2004

Makino, Hut et al. 2006

Glaschke, Amaro-Seoane, Sp, 2014a
Amaro-Seoane, Glaschke, Sp, 2014b

Software

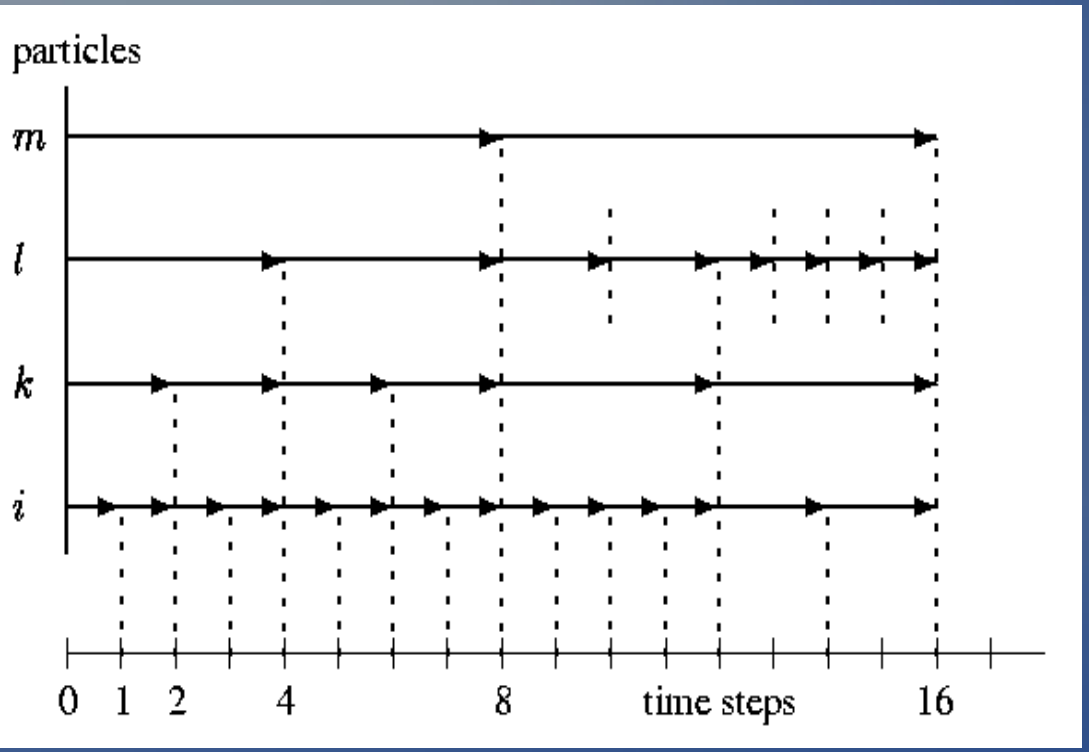

S.J.Aarseth, S. Mikkola (ca. 20.000 lines):

- Hierarchical Block Time Steps
- Ahmad-Cohen Scheme
- Regularisations
- 4th order Hermite scheme

- NBODY6 (Aarseth 1999)
- NBODY6++ (Spurzem 1999) MPI
- NBODY6++GPU (Wang, Spurzem, Aarseth et al. 2015)

Hierarchical Block Time Steps

$$\Delta t = \sqrt{\eta \frac{|\vec{a}||\vec{a}^{(2)}| + |\dot{\vec{a}}|^2}{|\dot{\vec{a}}||\vec{a}^{(3)}| + |\vec{a}^{(2)}|^2}} \,.$$

NBODY1 – NBODY7: “The Growth of an Industry” (Aarseth 1999)

	ITS	ACS	KS	HITS	PN	AR	CC	MPI	GPU
NBODY1	✓								
NBODY2		✓		✓					
NBODY3	✓		✓						
NBODY4			✓	✓					
NBODY5	✓	✓	✓						
NBODY6		✓	✓	✓					
NBODY6GPU		✓	✓	✓				✓	
NBODY6++		✓	✓	✓			✓		
NBODY6++GPU		✓	✓	✓	✓		✓	✓	✓
NBODY7		✓	✓	✓	✓	✓			✓

ITS: Individual time–steps [107]
ACS: Ahmad-Cohen neighbour scheme [109]
KS: KS–regularization of few-body subsystems [104]
HITS: Hermite scheme integration method combined with hierarchical block time-steps [111]
PN: Post-Newtonian [150, 125, 151]
AR: Algorithmic regularization [125]
CC: Classical chain regularization [114]
MPI: Message Passing Interface, multi-node multi-CPU parallelization [139]
GPU: use of GPU acceleration [138] (if also MPI: multi-node many GPU [144])

Berczik, Spurzem, et al., LNCS 2013; Table from: Spurzem, Kamlah 2023, LRCA

NBODY6++GPU: https://github.com/nbody6ppgpu/

Part of https://www.punch4nfdi.de/ PUNCH4NFDI Consortium w. Jülich

Table 5.1: Table showing important algorithmic, hardware and software development stepping stones in the development of direct N-body codes. The table is adapted from Aarseth (1999a), corrected in some places, but expanded to more recent developments.

Year	Keyword	Reference
1961.....	Force polynomial	(Aarseth, 1963)
	Individual time steps	(Aarseth, 1963)
	Gravitaitonal softening	(Aarseth, 1963)
1966.....	Spherical harmonics	(Aarseth, 1967)
1969.....	Two-body regularization	(Kustaanheimo & Stiefel, 1965)
1972.....	Three-body regularization	(Aarseth & Zare, 1974)
1973.....	Global regularization	(Heggie, 1974)
	Neighbor scheme	(Ahmad & Cohen, 1973)
1978.....	Co-moving coordinates	(Aarseth, 1979)
1979.....	Regularized AC	(Aarseth, 1985)
1980.....	Planetary formation	(Lecar & Aarseth, 1986)
1986.....	Hierarchical block-time steps	(McMillan, 1986)
1989.....	Chain regularization	(Mikkola & Aarseth, 1990)
1990.....	Particle in box scheme	(Aarseth, Lin, & Palmer, 1993)
1991.....	Collisional tree code	(McMillan & Aarseth, 1993)
1992.....	Chain N-body interface	(Aarseth, 1994)
1993.....	Hermite integration	(Makino, 1991)
1995.....	Synthetic stellar evolution	(Tout et al., 1997)
	Tidal circularization	(Mardling, 1995a, 1995b)
	Slow chain regularization	(Mikkola & Aarseth, 1998)
1996.....	Hierarchical stability	(Mardling & Aarseth, 1999)
1998.....	Evolution of hierarchies	(Mardling & Aarseth, 1999)
	Stumpff KS method	(Mikkola & Aarseth, 1998)
1999.....	HARP-6 procedures	(Aarseth, 1999a)
	Sympletic integrators	(Mikkola & Tanikawa, 1999b, 1999a)
	NBODY6++ SPMD / MPI acceleration	(Spurzem, 1999)
2000.....	Single stellar evolution - SSE	(Hurley, Pols, & Tout, 2000)
2002.....	Binary stellar evolution - BSE	(Hurley, Tout, & Pols, 2002)
2003.....	GRAPE-6 procedures	(Makino et al., 2003)
2006.....	2.5PN in NBODY5	(Kupi, Amaro-Seoane, & Spurzem, 2006)
2007.....	direct N-body GPU acceleration	(Portegies Zwart, Belleman, & Geldof, 2007)
2008.....	AR with Post-Newtonian terms	(Mikkola & Merritt, 2008)
2010.....	Updated AR for few-body problems	(Hellström & Mikkola, 2010)
2012.....	NBODY codes GPU acceleration	(Nitadori & Aarseth, 2012)
2013.....	MPI acceleration on GPU clusters / PHIGPU	(Berczik et al., 2013)
	3.5PN in NBODY6	(Brem, Amaro-Seoane, & Spurzem, 2013)
2015.....	SSE/AVX acceleration on GPU clusters	(Wang et al., 2015)
2017.....	Sympletic integrators (FSI)	(Dehnen & Hernandez, 2017)
2020.....	P^3T with SDAR in PETAR	(Wang, Nitadori, & Makino, 2020a; Wang et al., 2020a)
2021.....	Minimum spanning tree MSTAR/BIFROST	(Rantala, Naab, & Springel, 2021)

From:
Spurzem, Kamlah, Living Review Computational Astrophysics Vol. 9, pp. 3-109 2023

Parameterized stellar evolution tracks (IFMR for neutron stars and white dwarfs)

(SSE++/BSE++ from Kamlah et al. 2022 and Spurzem & Kamlah, Living Reviews Comp. Astroph. 2023)

- updated metallicity dependent core-collapse SNe, their remnant masses and fallback (Fryer et al. 2012; Banerjee et al. 2020),
- updated electron-capture supernovae (ECSNe), accretion-induced collapse (AIC) and merger-induced collapse (MIC) remnant masses and natal kicks (Nomoto 1984, 1987; Nomoto & Kondo 1991; Saio & Nomoto 1985, 2004; Kiel et al. 2008; Gessner & Janka 2018)
- (P)PISNe remnant masses (Belczynski et al. 2010, 2016; Woosley 2017),
- updated fallback-scaled natal kicks for NSs and BHs (Fuller et al. 2003; Scheck et al. 2004; Fryer 2004; Fryer & Kusenko 2006; Meakin & Arnett 2006, 2007; Fryer & Young 2007; Scheck et al. 2008; Fryer et al. 2012; Banerjee et al. 2020),
- and BH natal spins (see also Belczynski et al. (2020); Belczynski & Banerjee (2020)) from
  - `Geneva` model (Eggenberger et al. 2008; Ekström et al. 2012; Banerjee et al. 2020; Banerjee 2021b),
  - `MESA` model (Spruit 2002; Paxton et al. 2011, 2015; Banerjee et al. 2020; Banerjee 2021b),
  - and the `Fuller` model (Fuller & Ma 2019; Fuller et al. 2019; Banerjee et al. 2020; Banerjee 2021b).

ECSN = electron capture Supernova

AIC = accretion induced collapse

MIC = merger induced Collapse

PISN = pair instability Supernova

PPISN = pulsating PISN

NS = neutron star

BH = black hole

MESA = recent stellar evolution model

Codes

Parallelization
Supercomputing
GPU Computing

Our own φGRAPE/GPU N-body code

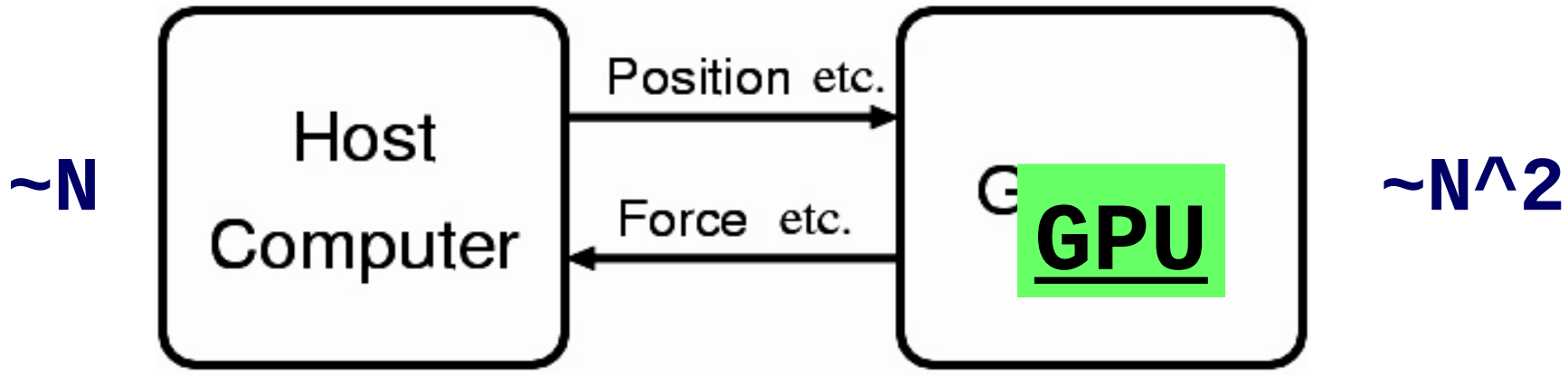

$$\vec{a}_i = \sum_{j=1;j\neq i}^{N} \vec{f}_{ij} \qquad \vec{f}_{ij} = -\frac{G \cdot m_j}{\left(r_{ij}^2 + \varepsilon^2\right)^{3/2}} \vec{r}_{ij}$$

Slide: Peter Berczik

Our CPU/GPU N-body (AC) code

NBODY6++GPU

Wang, Spurzem, Aarseth, et al. 2015, 2016

→ Exaflop/s Huang, Berczik, Spurzem 2016

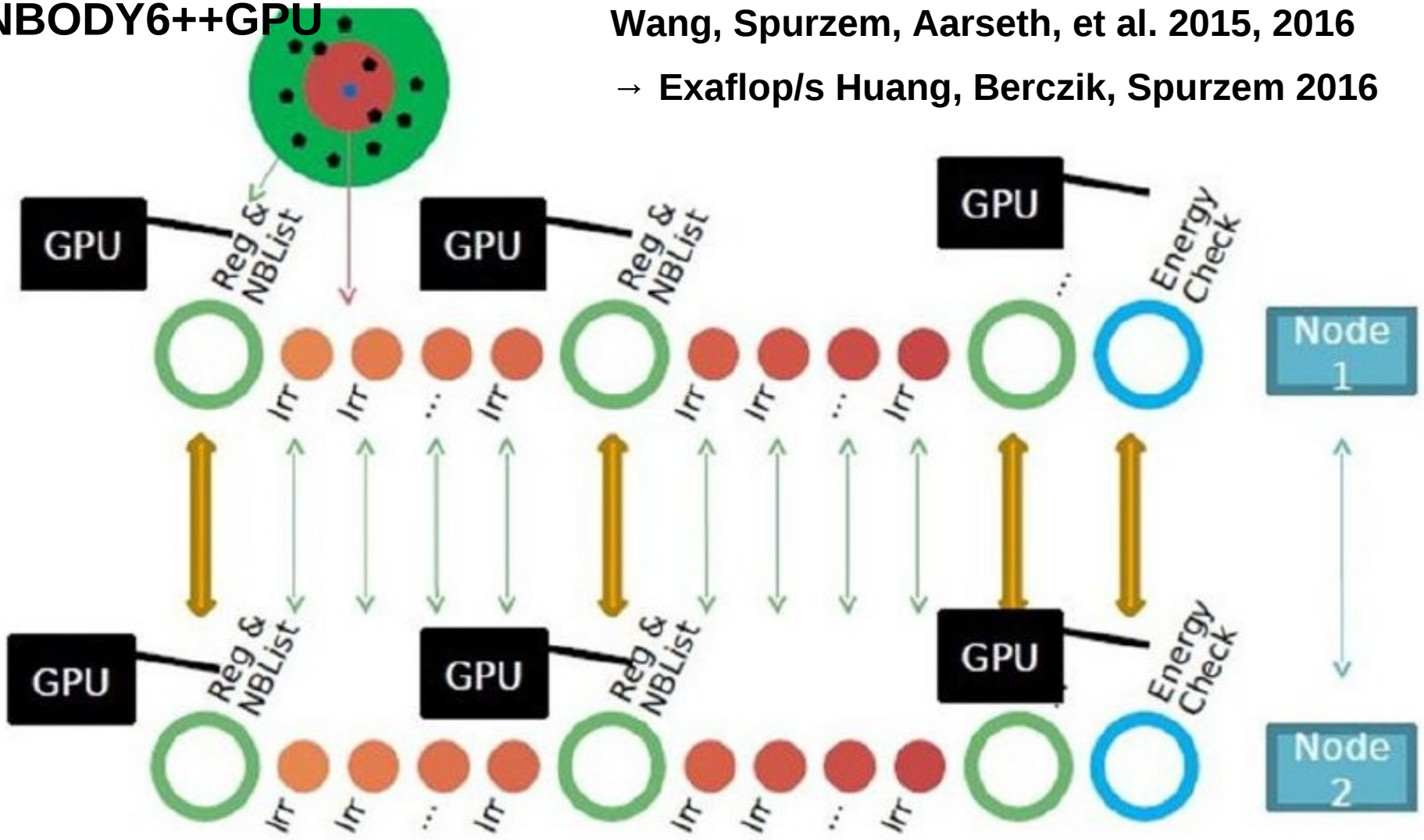

https://github.com/lwang-astro/betanb6pp

Table 5.1: Table showing important algorithmic, hardware and software development stepping stones in the development of direct N-body codes. The table is adapted from Aarseth (1999a), corrected in some places, but expanded to more recent developments.

Year	Keyword	Reference
1961.....	Force polynomial	(Aarseth, 1963)
	Individual time steps	(Aarseth, 1963)
	Gravitaitonal softening	(Aarseth, 1963)
1966.....	Spherical harmonics	(Aarseth, 1967)
1969.....	Two-body regularization	(Kustaanheimo & Stiefel, 1965)
1972.....	Three-body regularization	(Aarseth & Zare, 1974)
1973.....	Global regularization	(Heggie, 1974)
	Neighbor scheme	(Ahmad & Cohen, 1973)
1978.....	Co-moving coordinates	(Aarseth, 1979)
1979.....	Regularized AC	(Aarseth, 1985)
1980.....	Planetary formation	(Lecar & Aarseth, 1986)
1986.....	Hierarchical block-time steps	(McMillan, 1986)
1989.....	Chain regularization	(Mikkola & Aarseth, 1990)
1990.....	Particle in box scheme	(Aarseth, Lin, & Palmer, 1993)
1991.....	Collisional tree code	(McMillan & Aarseth, 1993)
1992.....	Chain N-body interface	(Aarseth, 1994)
1993.....	Hermite integration	(Makino, 1991)
1995.....	Synthetic stellar evolution	(Tout et al., 1997)
	Tidal circularization	(Mardling, 1995a, 1995b)
	Slow chain regularization	(Mikkola & Aarseth, 1998)
1996.....	Hierarchical stability	(Mardling & Aarseth, 1999)
1998.....	Evolution of hierarchies	(Mardling & Aarseth, 1999)
	Stumpff KS method	(Mikkola & Aarseth, 1998)
1999.....	HARP-6 procedures	(Aarseth, 1999a)
	Sympletic integrators	(Mikkola & Tanikawa, 1999b, 1999a)
	NBODY6++ SPMD / MPI acceleration	(Spurzem, 1999)
2000.....	Single stellar evolution - SSE	(Hurley, Pols, & Tout, 2000)
2002.....	Binary stellar evolution - BSE	(Hurley, Tout, & Pols, 2002)
2003.....	GRAPE-6 procedures	(Makino et al., 2003)
2006.....	2.5PN in NBODY5	(Kupi, Amaro-Seoane, & Spurzem, 2006)
2007.....	direct N-body GPU acceleration	(Portegies Zwart, Belleman, & Geldof, 2007)
2008.....	AR with Post-Newtonian terms	(Mikkola & Merritt, 2008)
2010.....	Updated AR for few-body problems	(Hellström & Mikkola, 2010)
2012.....	NBODY codes GPU acceleration	(Nitadori & Aarseth, 2012)
2013.....	MPI acceleration on GPU clusters / PHIGPU	(Berczik et al., 2013)
	3.5PN in NBODY6	(Brem, Amaro-Seoane, & Spurzem, 2013)
2015.....	SSE/AVX acceleration on GPU clusters	(Wang et al., 2015)
2017.....	Sympletic integrators (FSI)	(Dehnen & Hernandez, 2017)
2020.....	P^3T with SDAR in PETAR	(Wang, Nitadori, & Makino, 2020a; Wang et al., 2020a)
2021.....	Minimum spanning tree MSTAR/BIFROST	(Rantala, Naab, & Springel, 2021)

From:
Spurzem, Kamlah, Living Review Computational Astrophysics Vol. 9, pp. 3-109 2023

Parameterized stellar evolution tracks
(IFMR for neutron stars and white dwarfs)
(SSE++/BSE++ from Kamlah et al. 2022 and Spurzem & Kamlah, Living Reviews Comp. Astroph. 2023)

- updated metallicity dependent core-collapse SNe, their remnant masses and fallback (Fryer et al. 2012; Banerjee et al. 2020),
- updated electron-capture supernovae (ECSNe), accretion-induced collapse (AIC) and merger-induced collapse (MIC) remnant masses and natal kicks (Nomoto 1984, 1987; Nomoto & Kondo 1991; Saio & Nomoto 1985, 2004; Kiel et al. 2008; Gessner & Janka 2018)
- (P)PISNe remnant masses (Belczynski et al. 2010, 2016; Woosley 2017),
- updated fallback-scaled natal kicks for NSs and BHs (Fuller et al. 2003; Scheck et al. 2004; Fryer 2004; Fryer & Kusenko 2006; Meakin & Arnett 2006, 2007; Fryer & Young 2007; Scheck et al. 2008; Fryer et al. 2012; Banerjee et al. 2020),
- and BH natal spins (see also Belczynski et al. (2020); Belczynski & Banerjee (2020)) from
  - `Geneva` model (Eggenberger et al. 2008; Ekström et al. 2012; Banerjee et al. 2020; Banerjee 2021b),
  - `MESA` model (Spruit 2002; Paxton et al. 2011, 2015; Banerjee et al. 2020; Banerjee 2021b),
  - and the `Fuller` model (Fuller & Ma 2019; Fuller et al. 2019; Banerjee et al. 2020; Banerjee 2021b).

ECSN = electron captur
Supernova
AIC = accretion induced
collapse
MIC = merger induced
Collapse

PISN = pair instability
Supernova
PPISN = pulsating PISN

NS = neutron star
BH = black hole

MESA = recent stellar
evolution model

PeTar: a high-performance N-body code for modeling massive collisional stellar systems

Long Wang,[1,2]★ Masaki Iwasawa,[2,3] Keigo Nitadori[2] and Junichiro Makino[2,4]
[1]*Department of Astronomy, School of Science, The University of Tokyo, 7-3-1 Hongo, Bunkyo-ku, Tokyo, 113-0033, Japan*
[2]*RIKEN Center for Computational Science, 7-1-26 Minatojima-minami-machi, Chuo-ku, Kobe, Hyogo 650-0047, Japan*
[3]*National Institute of Technology, Matsue College, 14-4, Nishi-ikuma-cho, Matsue, Shimane 690-8518, Japan*
[4]*Graduate School of Science, Kobe University, 1-1 Roku...ho, Nada-ku, Kobe, Hyogo 657-8501, Japan*

Accepted XXX. Received YYY; in original form ZZZ

New competition 1:
PeTar: MNRAS 2020
Many more papers...

ABSTRACT
The numerical simulations of massive collisional stellar systems, such as globular clusters (GCs), are very time-consuming. Until now, only a few realistic million-body simulations of GCs with a small fraction of binaries (5%) have been performed by using the NBODY6++GPU code. Such models took half a year computational time on a GPU based super-

FROST: a momentum-conserving CUDA implementation of a hierarchical fourth-order forward symplectic integrator

Antti Rantala[1]★, Thorsten Naab[1], Volker Springel[1]
[1]*Max-Planck-Institut für Astrophysik, Karl-Schwarzschild-Str. 1, D-85748, Garching, Germany*

New competition 2:
FROST: MNRAS 2021
BIFROST: MNRAS 2022

Accepted XXX. Received YYY; in original form ZZZ

ABSTRACT
We present a novel hierarchical formulation of the fourth-order forward symplectic integrator and its numerical implementation in the GPU-accelerated direct-summation N-body code FROST. The new integrator is especially suitable for simulations with a large dynamical range due to its hierarchical nature. The strictly positive integrator sub-steps in a fourth-

NBODY6++GPU with up to 16M particles

(Benchmarks on raven at MPCDF)

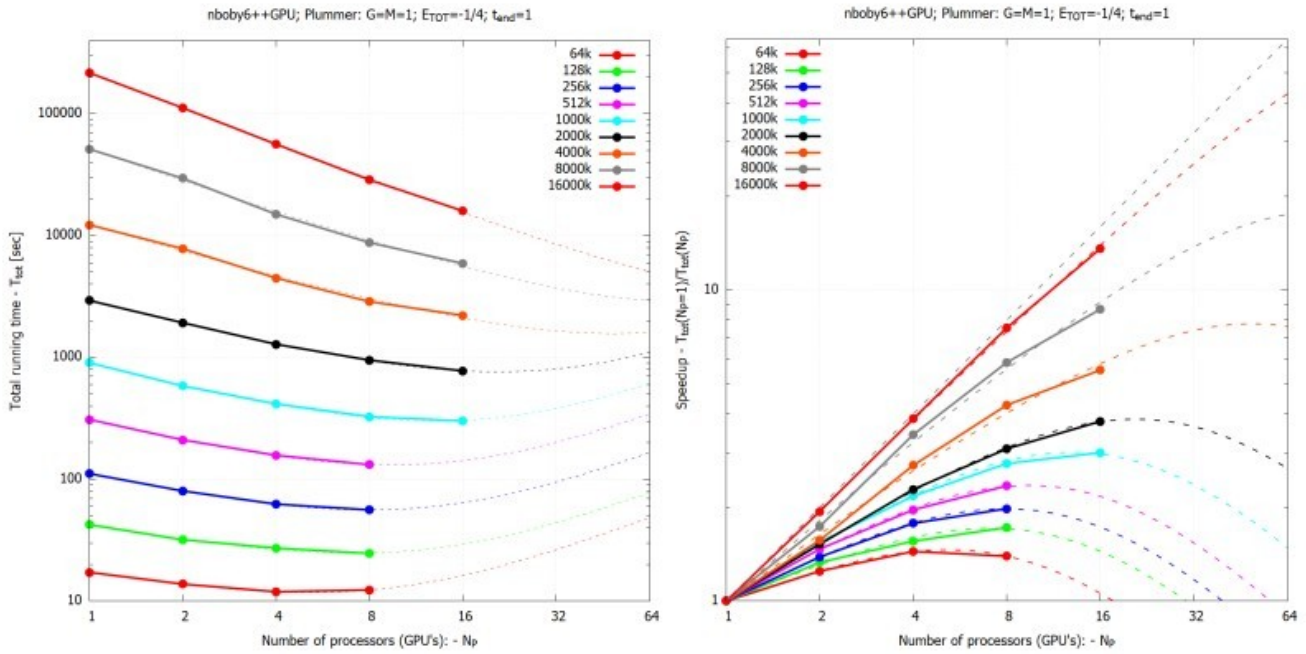

Figure 6: Benchmark results and extrapolated scaling for NBODY6++GPU, initial Plummer model, on the raven cluster at MPCDF, see main text. **Left:** Total time for one NBODY model unit in secs; **Right:** Speed-Up compared to using one GPU only. In both cases different curves for particle numbers from 64k to 16m. Ideal Speedup is the diagonal dashed lines, other dashed lines extrapolations from the timing model.

Supercomputers

A special-purpose computer for gravitational many-body problems

Nature 1990

Daiichiro Sugimoto*, Yoshihiro Chikada†, Junichiro Makino*, Tomoyoshi Ito*, Toshikazu Ebisuzaki* & Masayuki Umemura‡

* Department of Earth Science and Astronomy, College of Arts and Sciences, University of Tokyo, 3–8–1 Komaba, Meguro-ku, Tokyo 153, Japan
† Nobeyama Radio Observatory, Minamimaki-mura, Minamisaku-gun, Nagano 384–13, Japan
‡ National Astronomical Observatory, Mitaka, Tokyo 181, Japan

A processor has been constructed using a 'pipeline' architecture to simulate many-body systems with long-range forces. It has a speed equivalent to 120 megaflops, and the architecture can be readily parallelized to make teraflop machines a feasible possibility. The machine can be adapted to study molecular dynamics, plasma dynamics and astrophysical hydrodynamics with only minor modifications.

(very-large-scale
puter is construc
lem is to devel
construction and
of physical syste
to these apparent
ted in the compu
GRAPE-1 achie
XMP/1 at a cos

The pipeline a

The N-body pro

GRAPE-6 Gravity/Coulomb Part

- G6 Chip: 0.25μ 2MGate ASIC, 6 Pipelines
- at 90MHz, 31Gflops/chip
- 48Tflops full system (March 2002)
- Plan up to 72Tflops full system (in 2002)
- Installed in Cambridge, Marseille, Drexel, Amsterdam, New York (AMNH), Mitaka (NAO), Tokyo, etc..

Jun Makino with GRAPE6 → (2002)

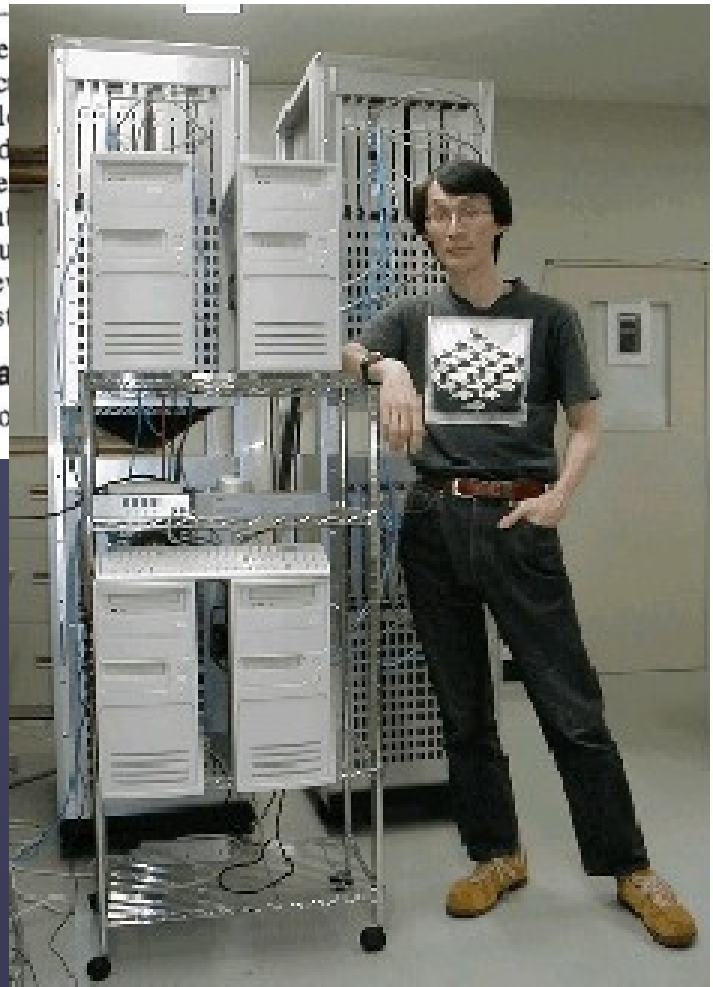

NAOC laohu cluster

64 Kepler K20

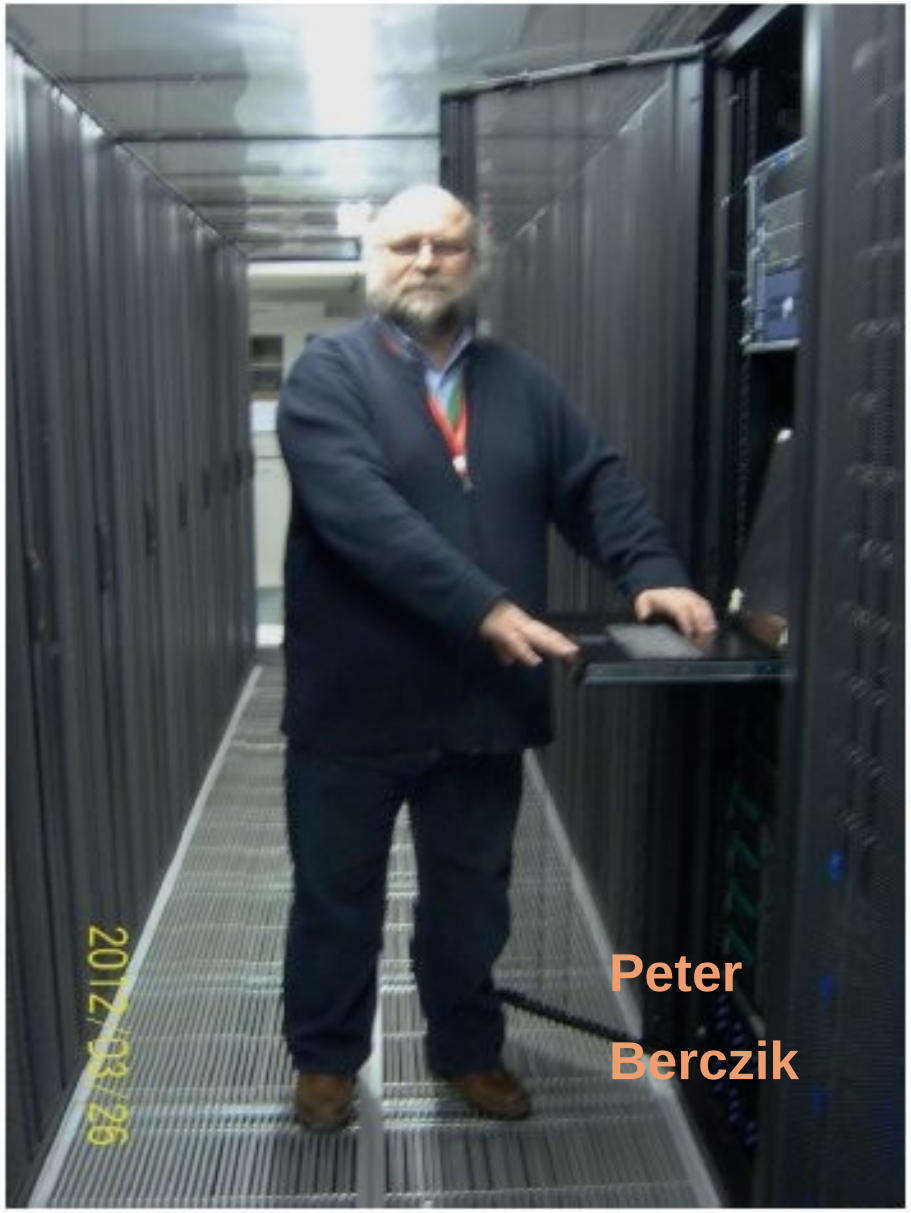

Laohu: 2009/2015

(Kepler GPU)

100 Tflop/s 150k cores

New GPUs 5-6 times faster… (see below)

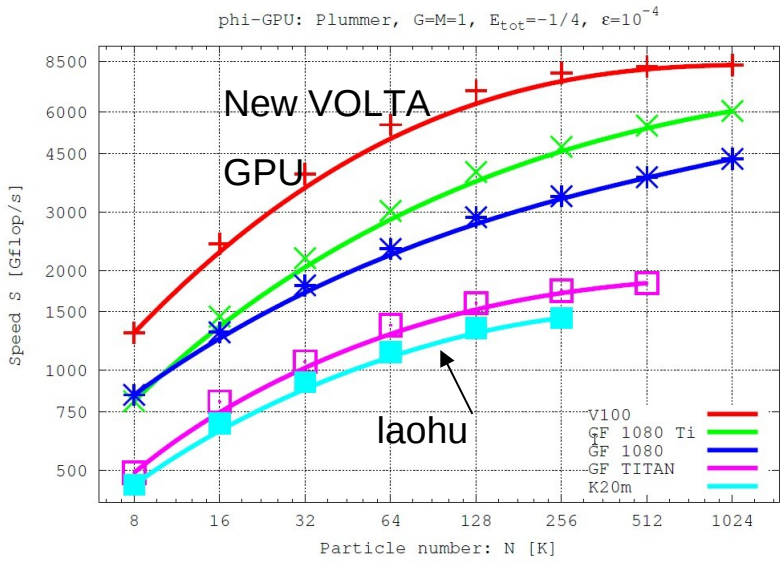

GCS
Gauss Centre for Supercomputing

JUWELS Booster 936 nodes (AMD CPU, 4x Ampere GPU)

~450.000 AMD cores, 25 million NVIDIA Ampere GPU cores

~ 70 Pflop/s SP ~ 44 Pflop/s DP

No. 12 in top500 list, No. 25 in green500 list

Jülich Wizard for European Leadership Science

Copyright:
— Forschungszentrum Jülich

LUMI

Supercomputer, Kajaani, Finland

Using only

Hydroelectric

Power and its

Heat used for heating buildings.

No. 3 in top500

No. 7 in green500

2.2 million cores

10.000 AMD GPUs

EuroHPC and LUMI consortium:

Finland, Belgium, Czech Republic, Denmark, Estonia, Iceland, Norway, Poland, Sweden, and Switzerland.

China New Computing Technology

V100的全面国产替代 ——海光DCU Z100L 面向人工智能的GPGPU加速卡

mzzy
服务器厂家

简单介绍一下海光的这款产品

DCU (Deep Computing Unit) Z100L 是一款面向人工智能、科学计算的高性能全功能GPGPU加速卡。

规格参数		Z100L及Z100L-LP	
应用场景		全精度支持	AI优化
适配服务器		2U/4U风冷服务器	
构架核心	计算核心	3840	
	频率	1319MHz	1600MHz
性能指标	FP64	10.1TFlops	——
	FP32	10.1TFlops	12.2TFlops
	FP16	20.2TFlops	24.5TFlops
	INT8	40.5TFlops	49.1TFlop
存储规格	显存容量	32GB HBM2	
	显存带宽	1024 GB/s	
接口类型	PCIe 接口	PCIe 4.0 x16	
	GPU 互联	xHMI互联 184GB/s	
最大功耗	TDP	250W	280W
尺寸规格	尺寸	全高全长双宽	

知乎 @rnzzy

Hygon CPU/DCU
(Deep Computing Unit)

~ AMD EPYC/AMD GPU
HIP programming language

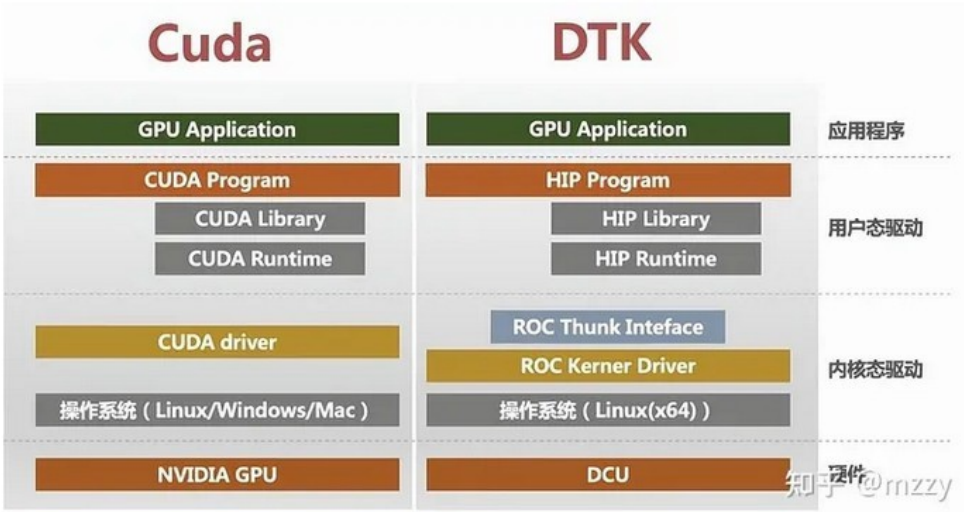

CUDA数学库	DTK数学库	数学库功能
cudnn	miopen	深度学习基础数学库
cublas	rocblas/hipblas	基础矩阵运算数学库
nccl	rccl	通信库

FESENKOV ASTROPHYSICAL INSTITUTE

China-Aid HPC Solution for FAI

China – Kazakhstan government funded science collaboration (several disciplines)

Astrophysics: Silk Road NAOC with FAI

50 GPU Servers (~400 GPUs), Storage, Network, …

Use Chinese Hardware

1) Star Cluster Simulations/
   Black Holes/Grav. Waves
2) Nuclear Star Clusters
3) Code(s) and Hardware
4) **Summary and References**

DRAGON I Simulation: Wang, Spurzem, Aarseth, et al. 2015, 2016

DRAGON II Simulation: Arca Sedda, Kamlah, Spurzem, et al. 2023, 2024ab

DRAGON III Simulation: Wu et al. 2025, in prep., and DRAGON Data Release

https://github.com/nbody6ppgpu

The Future - DRAGON III 1m – 8m (16m?)

- Compare and validate, also with other methods (MOCCA, CMC, Fokker-Planck, ...)
- Globular Cluster (GC) next issues: Rotation, Populations, Tides and Tails, …
- Nuclear Star Cluster (NSC) Simulations: TDE, EMRI, direct capture, partial TDE, partial accretion to SMBH.
- Will legacy codes survive with good support? (Ease of use, data releases, interfaces, new modules…)
- AI assisted coding, how far will it go?

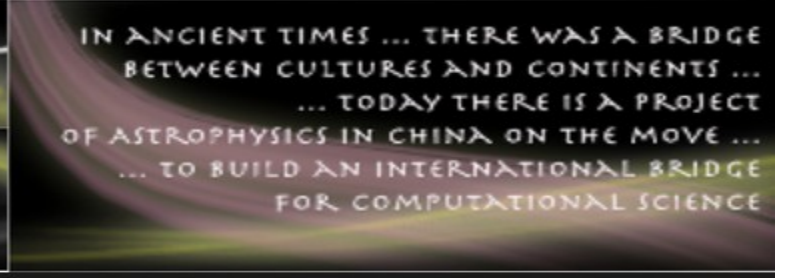

Silk Road Conference (former KCK - Kazakhstan, China, Korea, Uzbekistan Meeting)

14th Silk Road Conference

2nd Meeting of the Silk Road Astronomy Research and Education Alliance, Silk Road AREA

Exploring the Frontiers of Dynamical Astronomy with High-Performance Computing, Artificial Intelligence, and Leading-Edge Observational Techniques.

We continue the numbering of these conferences, which started as Korea-China meeting in 2009; later it became Kazakhstan-China-Korea meeting, and due to increasing interest and participation of colleagues from all over central and east Asia we decided now to rename it to Silk Road Conference.

New Uzbekistan University, Tashkent, Uzbekistan, May 18-22, 2026.

Last Conference: 13th Silk Road / 1st Silk Road AREA meeting

Scientific Organizing Committee*: https://astro-silkroad.eu/conferences/silkroad14

Zhongmu Li (Dali U), Rainer Spurzem (ARI/ZAH, NAOC/CAS, KIAA/PKU)

Bobomurat Ahmedov (ITP, IAS, IFAR, UBAI, HAI)

Kanat Baigarim (ECL/NU), Chingis Omarov (FAI),

Ernazar Abdikamalov (ECL/NU), Bekdaulet Shukirgaliyev (ECL/NU)

Hyung Mok Lee (SNU)

Thijs (M.B.N.) Kouwenhoven (XJTLU)

ARI ITA LSW

Team & Collaborators as below and further:

Thorsten Naab (MPA), Mirek Giersz (CAMK),
Ataru Tanikawa (Tokyo U), Nadine Neumayer (MPIA)

DRAGON simulations – globular and nuclear star clusters

- **DRAGON simulation: PhD thesis Long Wang, KIAA/PKU,** awarded for first realistic globular cluster simulation using **NBODY6++GPU** with one million stars and many binaries (Wang, Spurzem, Aarseth, et al., MNRAS 2016).
- **The Dragon-II simulations – Paper III. Compact binary mergers in clusters with up to 1 million stars: mass, spin, eccentricity, merger rate and pair instability supernovae rate** (Arca Sedda, M., Kamlah, A. W. H., Spurzem, R., et al.) **Paper I,II,III (MNRAS 2023, 2024)**

NBODY6++GPU and more, current state:

- **Spurzem, R., Kamlah A.W.H. Direct N-body simulations, in Living Rev. in Comp. Astrophysics 9, id.3 (2023) (NBODY7 see also Banerjee, Sambaran papers)**

Direct Nuclear Star Cluster Models with SMBH and TDE:

- **DRAGON simulation of the Galactic Center**, PhD thesis of Taras Panamarev, ARI/ZAH Univ. of Heidelberg (Panamarev, Just, Spurzem, Berczik, Wang, Arca Sedda, MNRAS 2019), simple TDE
- **Revisit the Rate of Tidal Disruption Events: The Role of the Partial Tidal Disruption Event** (Zhong, S., Li, S., Berczik, P., Spurzem, R.) 933, 96 (2022), TDE improved 3
- Marija Minzburg, Philip Cho: Master Thesises Heidelberg 2023, publication in progress, TDE improved 1 and 2, paper in preparation.

Recent or in prep.:

- Vergara et al. 2024, A&A, 2025, to be submitted A&A – Formation of IMBH
- Li, Zhong, Berczik, Spurzem, Chen, Liu (MNRAS 2023 and earlier): merging nuclei with TDE
- Amiri et al., fractal initial models, primordial mass segregation
- Kamlah, Wu, Liu, Tanikawa, Neumayer, Sp, et al., PopIII star clusters
- Cho, Wu, Sp et al., DRAGON-III of nuclear star clusters